UNIVERSITY of CAMBRIDGE

CENTRIFUGE MODELLING IN CLAY MARINE APPLICATIONS

by

S M Springman

CUED/D-SOILS/TR260 1993

Department of Engineering

TECHNICAL REPORT

**CENTRIFUGE MODELLING IN CLAY
MARINE APPLICATIONS**

by

S M Springman

CUED/D-SOILS/TR260 1993

This paper was originally published as a keynote address to the 4th Canadian Marine Geotechnical Conference in St Johns' Newfoundland in June 1993.

CENTRIFUGE MODELLING IN CLAY: MARINE APPLICATIONS

S. M. Springman Cambridge University Engineering Department
Trumpington Street, Cambridge, CB2 1PZ, UK

ABSTRACT

The advantages of centrifuge modelling compared with full scale field testing are particularly apparent when soil-structure interaction in offshore and marine applications is to be investigated. This paper will concentrate on how to prepare a model in clay, having designed a strength profile for the clay layer. Some typical stress paths obtained throughout the modelling will also be presented, together with an introduction to in-flight and post-test site investigation techniques.

IDEALISATIONS FROM MODEL TO PROTOTYPE

Modelling a field situation will always require some idealisation. Designers will tend to describe a variable matrix of rock and soil in terms of zones and layers, using some appropriate properties to allow analysis of their performance under some loading regime. The range of critical modes of behaviour will be identified and the factors which might affect them will be studied in detail.

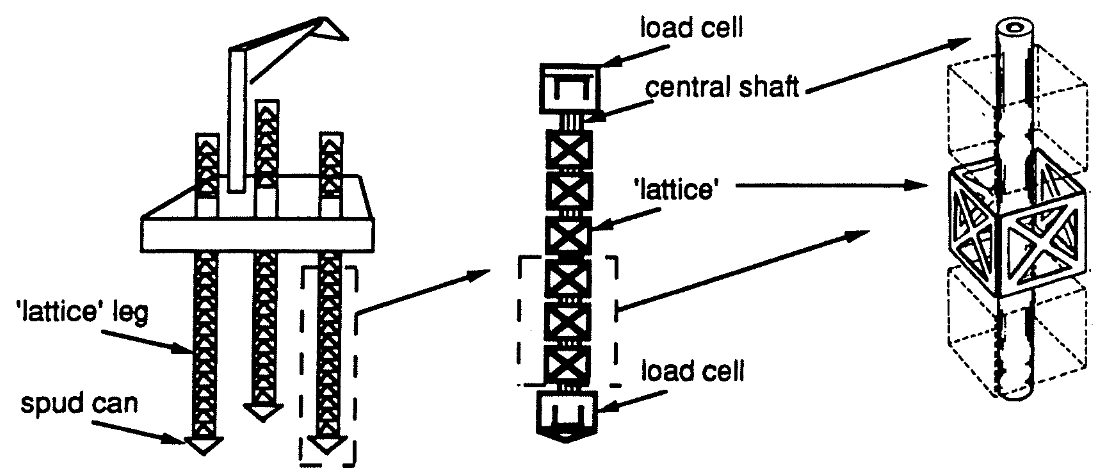

Figure 1a Jack up platform Figure 1b Idealisation Figure 1c 'Lattice' arrangement

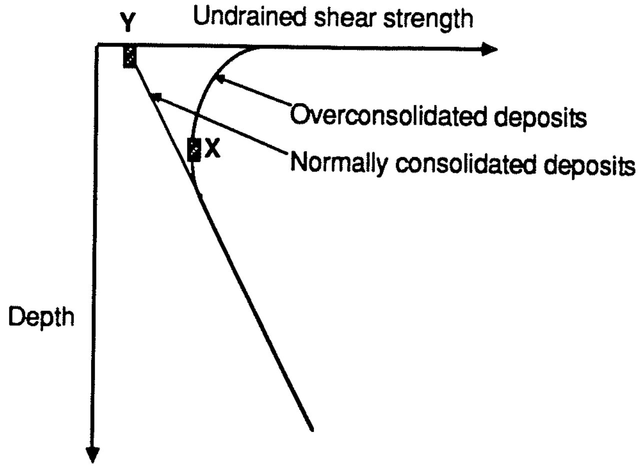

Figure 1d Typical undrained shear strength profile with depth

For example (Figure 1a), the behaviour of an offshore jack up platform could be described as a complex interaction between the rig, leg and spud geometry, depth of embedment in, and characteristics of, the founding stratum, and the dynamic wave and wind loading. In order to identify the basic controlling mechanisms, a jack up structure with three lattice legs (Figure 1a) might be replaced by a single leg with a central column of an equivalent, scaled, bending rigidity, which has been instrumented to allow an evaluation of the shear force and bending moment distribution (Figure 1b). To mimic the transfer of lateral load from the latticework to the surrounding soil, it is possible to mount plates which have an equivalent cross sectional area from fixings attached to the central shaft (Figure 1c).

Thus, intelligent simplifications will be used to replicate the important features which will control the pattern of behaviour in the prototype.

Idealisation may also deal with the soils to be used in the model. For clay deposits, there are several possibilities:

* to take undisturbed samples of 'prototype' soils, so that local structure is maintained, and naturally occurring preferential seepage paths remain (unsmeared),
* to remould the natural soil in some fashion,
* to use the most appropriate remoulded 'laboratory' soil (such as kaolin) for which there is an extensive database of properties.

Hight *et al.* (1985) comment on various sampling techniques for typical offshore clays, and the influence of this on subsequent soil behaviour. Small strain stiffness is often lost from normally consolidated block samples, and in addition, the peak strengths that might be expected in lightly overconsolidated blocks are not achieved. This effect is less noticeable in heavily overconsolidated samples. Clearly this is important if serviceability limit states and some associated geo-structural mechanisms are to be modelled correctly. In all cases the disturbance due to sampling appears to have been erased by the time that ultimate strengths are reached, provided the water contents do not change significantly.

Endicott (1970) and others have endeavoured to produce undisturbed samples from the field for use in centrifuge modelling - generally for embankment stability problems investigated on a beam centrifuge. However, the practicalities of sampling, transfer to the model and subsequent back analysis of the results did not give acceptable reproduction of the prototype performance, and this was for an onshore site. Sampling will be extremely expensive for offshore applications, and for sensitive or soft clays, may not be justified by the 'quality' of the sample obtained. If field samples are to be taken from an overconsolidated deposit, they should be sampled from the weakest stratum (Figure 1d; lowest value of c_u ; point X for overconsolidated clays, point Y for normally consolidated clays), so that subsequent stress fields imposed in the centrifuge may lead to the best approximation of the key field strength conditions, but in consequence, the strains will not be entirely comparable.

Horner (1982) used powdered Boston Blue clay, remixed under vacuum with distilled water, to predict the behaviour of an M.I.T. trial embankment, but this remoulded natural soil lacked the fabric (and probably the stress history and recent stress path) of the in-situ material and so the prediction was not good. Further discussion of the use of real or laboratory soils is included later in this paper.

For the general case of a jack up platform outlined in Figure 1a, the soil-structure interaction is controlled by the combination of strength and stiffness of the soft soil. Therefore, it is possible to isolate this aspect by replicating a typical strength profile (Figure 1d) in the centrifuge model and to observe the same mechanisms which lead to failure in the prototype.

CENTRIFUGE MODELLING

Marine applications

There are, of course, many possible modelling opportunities in clay for soil-structure interaction in a marine environment. They are particularly appropriate given the large size of most of these structures, the financial and technical investment required to mobilise these projects and, in consequence, the relative paucity of good quality site investigation data. Craig (1988) commented that the offshore and coastal engineering industries had benefitted more than most from centrifuge model testing in the development of current design methods.

Mechanisms observed, in clay, during aspects of behaviour of gravity platforms (Rowe, 1975), anchors, jack up spud cans (Craig and Chua, 1991; Springman 1991), monotonic and cyclic loading in an axial sense on tension piles (Nunez, 1989) and laterally on a variety of large tubular open ended piles (Hamilton *et al.*, 1991), suction piles and anchors (Fuglsang and Steensen-Bach, 1991; Renzi *et al.*, 1991), seabed mechanics and many other applications have been investigated using beam centrifuges around the world.

Thermal influences, such as those caused by sub-seabed disposal of high level radioactive waste, have been examined by Savvidou (1984). A heat source buried in a deep clay layer generated pore pressure and caused cracking due to the differential thermal coefficients of expansion of both the soil and fluid phases. Her analysis considered the coupling of heat and fluid flow. Poorooshasb (1988) took this investigation one step further by firing projectiles of differing shapes into a soft clay layer and then heating the environment around which the projectile came to rest. The primary question was whether a gap would be left behind the projectile, creating a preferential leakage path or whether the soil would deform in a sufficiently plastic fashion to close that gap. The effect of heat on this region was found to increase the likelihood of leakage along this softened zone due to thermal cracking.

At the other extreme, cold regions engineering will be important to the new facility at CCore. Previous work at Cambridge has largely focussed on the influence of ice forces on offshore structures (Vinson, 1982; Lovell, unpublished) or iceberg scour above pipelines buried below the seabed (Lach, 1992). Experiments in which the ground has been frozen have been concentrated in mainly onshore applications. Smith (1992) investigated the thaw-induced settlement of pipelines and Vinson (1983) discussed the effect of hot fluids flowing through pipelines in frozen ground.

There are few studies on the response to earthquake excitation for structures built on clay. The difficulties of reconciling scaling laws for diffusion time and inertial time necessitate the use of a more viscous pore fluid, which is complicated in fine grained clayey soils. Similarly, the centrifuge is not best suited to examining chemical effects on soil deposits.

A different style of centrifuge, in which a 1 m diameter drum may be rotated, in the extreme limit at 670 rpm, to present a seabed of 0.5 km by 3 km in a gravity field of 500 g, has allowed examination of the installation and response to a variety of axial, lateral and moments on a 3-legged jack up rig mounted on spud cans (Wong *et al.*, 1993). Carefully prepared block samples of clay were inserted into a sand base at the site of the rig installation. This procedure will not be described in this paper, which will concentrate primarily on the type of models prepared for a beam centrifuge such as the new Acutronic 680-2 recently installed at CCore in St John's, Newfoundland.

Scaling effects

Stress and strain

Centrifuge modelling techniques are particularly advantageous when comparing the behaviour of non-linear materials in small and full scale prototypes of soil-structure interaction problems. It is vital that the correct stress-strain fields are replicated if meaningful interpretation is to be obtained. Similarity of stress and strain will be achieved in both model and prototype, for a sample constructed at a scale of $1/n$, located at an appropriate radius and rotated at an angular velocity to give a multiple of earth's gravity, n g at that radius. Schofield (1980) discusses the scaling laws in detail, together with the range and magnitude of possible errors.

Table 1 Comparison between the use of real or laboratory soils in centrifuge model tests

Activity	*Field prototype soil*	*Laboratory alternative soil*
Aim	To reproduce the exact soil behaviour from the field in the centrifuge model.	To model the relevant prototype soil behaviour using a known laboratory soil.
Sampling and disturb-ance	Inserting a cutter to extract a block sample, preparation for transport and subsequent trimming to fit a centrifuge strongbox, is likely to cause softening and loss of peak strength (the extent depending on OCR of the soil). Disturbance will be significant.	Mixed from a slurry under vacuum, consolidated in a liner and consolidometer before transfer of the liner containing the soil to the centrifuge strongbox. The sample is assumed to be uniform and homogeneous in stress state and properties. Disturbance is not likely to be a problem.
Local structure	If this exists, then it is difficult to quantify and is likely to confuse back analysis of model test.	No local cementation exists; critical states may be adopted to explain soil behaviour.
Aging	Local cementation, particle shape variations, load cycling - will be disturbed during sampling, and are difficult to model.	The repetition of 1g - ng loading cycles appears to cause a slight increase in strength. Further research is underway at the moment.
Particle size	For soil deposits which contain random large particles, it should be remembered that these will be enlarged by a factor of n with respect to the model dimensions. Therefore, shell fragments in remoulded calcareous deposits assume a reinforcing role out of proportion to the rest of the soil layer, and should be removed. Root systems in naturally occurring clays may become major tunnel networks.	The size of any structure / probe acting on granular soil particles of mean diameter, d should be > 12 d (Phillips and Valsangkar, 1987), so this value may be less in clay. The same field and model particle size/void ratio/pore fluid will not affect permeability. Time taken for dissipation of excess pore pressures (diffusion) will be n^2 faster. Sometimes pore fluid with n times higher viscosity may be used so that both diffusion / inertial velocity will be factored by n.
Permea-bility	Impermeable natural clays (e.g. montmorill-onite) take lengthy consolidation time at n g.	Relatively permeable clays such as kaolin may be used to minimise consolidation time.
Homogen-eity	Unless the sample is remoulded, it is difficult to assess this until after the test.	This is completely controlled in the centrifuge sample.
Heterogen-eity	The field sample is more likely to be anisotropic.	1d consolidation: no radial strain at sample boundaries; stress field assumed to be uniform.
Properties	Exhaustive sets of laboratory tests may be necessary to establish the soil parameters for design of test and subsequent back analysis.	Extensive databases exist for this soil. Class-ification and extra laboratory tests using appropriate stress paths may be carried out.
Stress history	Undisturbed samples will retain the stress history and sampling effects at the nominal depth of sampling +/- 200mm. The centrifuge model will reproduce stress history for n times the depth of real samples, from ground surface downwards. The prototype may have been subjected to differing stress histories and paths.	This may be designed to suit the requirement of strength and stiffness with depth, remembering that the sample is consolidated at 1g under uniform total stress. The effective stress profile may be manipulated by using upward / downward hydraulic gradients to create a linear pore pressure profile.
Global structure	Samples taken from one or a small number of depths do not represent the global variation of OCR, strength and stiffness with depth.	Realistic variation of some properties (e.g. OCR) with depth, but less realism in others (e.g. anisotropy).
Results	Distortion of global effects due to samples not representing fully the in-situ soils.	Global effects modelled better except that soil properties may be different from the field soil.
Conclusion	Direct scaling from model to prototype possible in rare instances only. Usually, model data needs to be understood in an analytical framework, which is then applied to the field situation.	

Consolidation - time

In the centrifuge, the scaling factor for modelling time in terms of diffusion may be demonstrated to be $1/n^2$ (Schofield, 1980). Non-dimensional time factor, $T_v = f$ [time/(depth)^2], will be unaffected by gravity level for a depth of sample reduced to $1/n$ of the original, if the model time is also reduced, but by $1/n^2$. This is significant for tests using clay because the prototype consolidation times would be prohibitive: 27 years of prototype diffusion may be modelled in 1 day using a centrifuge at 100 g.

Representation of field samples

In general, a well known and understood 'laboratory' soil such as kaolin may be preferable to choosing a soil taken from the field. Table 1 examines some of the issues.

This paper focusses on current practice for preparing centrifuge models in clay using kaolin and considers the potential use of kaolin mix soils.

Design of stress history

Soil behaviour in the future is a direct function of past stress history, together with the recent and anticipated stress path. Creating a centrifuge model sample in the laboratory allows control of both the stress history and the stress path due to one dimensional consolidation prior to model making, reconsolidation in the centrifuge and any subsequent loading. It is possible to design soil deposits which will exhibit a chosen range of strength and stiffness, although there are some anisotropic details which cannot be modelled effectively.

Various relationships have been proposed by Skempton (1957), Bjerrum (1973), and Lerouil *et al.* (1985) to link undrained shear strength c_u, and effective vertical stress in one dimensional normal compression (or preconsolidation pressure in an oedometer) σ_{vc}' via peak values obtained from field vane shear test results. However, these field strength ratios c_u / σ_{vc}' were found to be dependent on plasticity index I_p. When this aspect is accounted for, the variation of $c_{u\ vane}$ measured by the vane with back-analysed values of c_u at failure (when the factor of safety is unity), may be adjusted by Bjerrum's factor μ (Figure 2a).

The resulting field strength ratio is almost independent of plasticity (Muir Wood, 1990), with a roughly constant value (Figure 2b):

$$\mu\, c_{u\ vane} / \sigma_{vc}' = 0.22 \qquad \text{where} \qquad c_{u\ field} = \mu\, c_{u\ vane} \tag{1}$$

This has been confirmed by Trak *et al.* (1980) who suggested that the critical state (undrained) strength at large strains has a value of around 0.22, which is almost independent of plasticity. However, it should be noted that this is for *normal compression*, i.e. a normally consolidated clay.

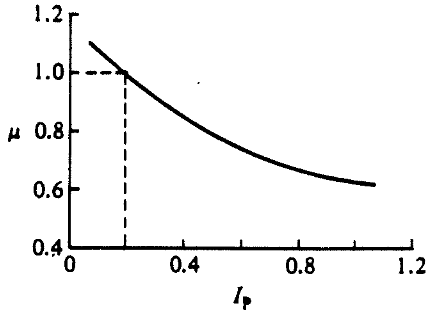

(a) correction factor, μ (Bjerrum, 1973)

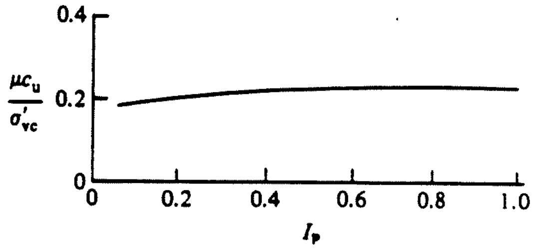

(b) $\mu\ c_{u\ vane} / \sigma_{vc}'$ v I_p (Mesri, 1975)

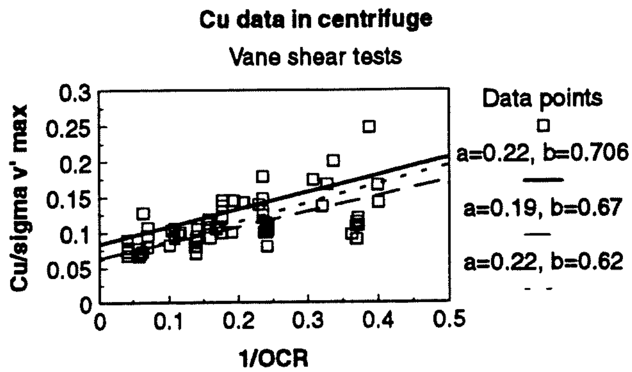

(c) data from centrifuge models

Figure 2 Empirical determination of c_u from vane shear strength data

When allowance is to be made for overconsolidation ratio OCR, then it was suggested by Schofield and Wroth (1968), that for the current effective vertical stress, σ_v' :

$$c_u / \sigma_v' = a\ OCR^{\ b} \qquad (2)$$

where a and b are constants. (For OCR = 1, Equation 2 reduces to Equation 1 with a = 0.22)

The effective stress profile in the consolidating sample is a major controlling factor. A 1 g consolidometer resembles a large scale laboratory oedometer of either rectangular (Figure 3a) or circular (Figure 3b) cross section. When a uniform total vertical stress σ_v is applied, with drainage to the same pore pressure u at the top and bottom of the sample, then the effective vertical stress σ_v' is likely to be almost constant (Figure 4a). When the centrifuge acceleration of n g is applied, the new vertical effective stress (after equalisation at n g) will define the OCR and hence the value of c_u .

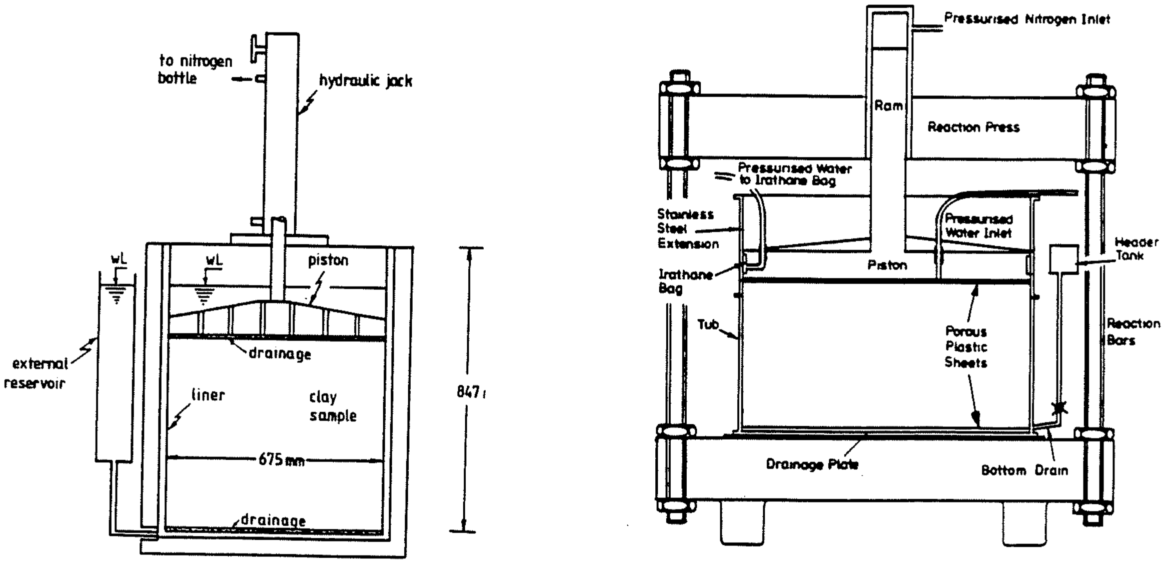

(a) plane strain (Almeida, 1984)

(b) axisymmetric with downward hydraulic gradient (Phillips, 1988)

Figure 3 1g consolidometer for centrifuge models in clay

Kaolin as a model soil

Strength

Vane shear tests conducted in-flight in the centrifuge have given data as shown in Table 2. A selection of results from 6 series of data by 5 researchers are plotted as symbols in Figure 2c, and the key ranges of a and b (described by * in Table 2) are drawn as lines. There is a significant scatter, possibly induced by different testing protocols (e.g. time to rotation).

Table 2 Constants for relating c_u to OCR and σ_v' for speswhite kaolin

Research worker	*Date*	*a*	*b*	*Comment*
Nunez	1989	0.22	0.62	*
Phillips	1987	0.19	0.67	*
Springman	1989	0.22	0.76	upper limit
			0.706	* mean
			0.62	lower limit

For example, a kaolin layer, 350 mm deep with a pre-consolidation vertical stress of 110 kPa will have an equivalent effective vertical stress of 110 kPa if the sample drains to an excess pore pressure of zero at the top and bottom of the sample (Figure 4a). Subsequent consolidation at 100 g in soil with $\gamma' = 6$ kN/m^3, will imply $\sigma_v' = 6 \times 0.35 \times 100 = 210$ kPa at the base of the sample: 0.35 x 100 = 35 m depth in the prototype. A 2nd stage consolidation may follow, in which the total vertical stress is increased to 225 kPa (Figure 4b) and a downward hydraulic gradient is introduced so that the pore pressure remains 165 kPa at the top of the consolidating sample, decreasing to zero at the base. The σ_v' profile is linear, showing 60 kPa at the surface and 225 kPa at the base.

A combined maximum vertical effective stress profile is given in Figure 4c, and this was used for the idealised jack up 'lattice leg' model tests. The OCR profile is then given for equilibrium at 100g, together with the ideal profile of c_u (Figure 5). The effective stress exceeds the previous maximum stress below model depths of 170 mm (17 m prototype; point X; Figure 5), where the OCR approaches unity. Below this, the predicted profile of c_u is linear with depth (Equation 2).

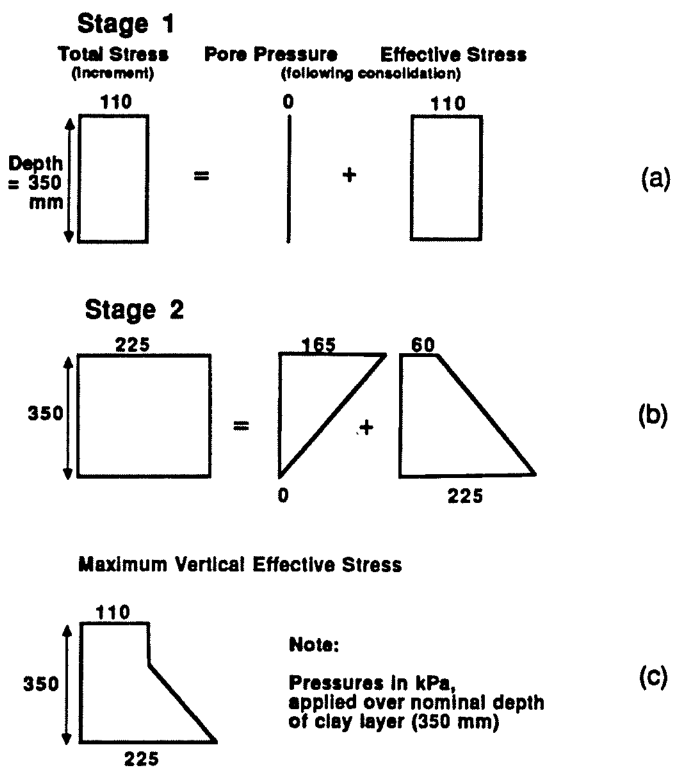

Figure 4 Development of stress history in a consolidometer at 1 g (Springman, 1991)

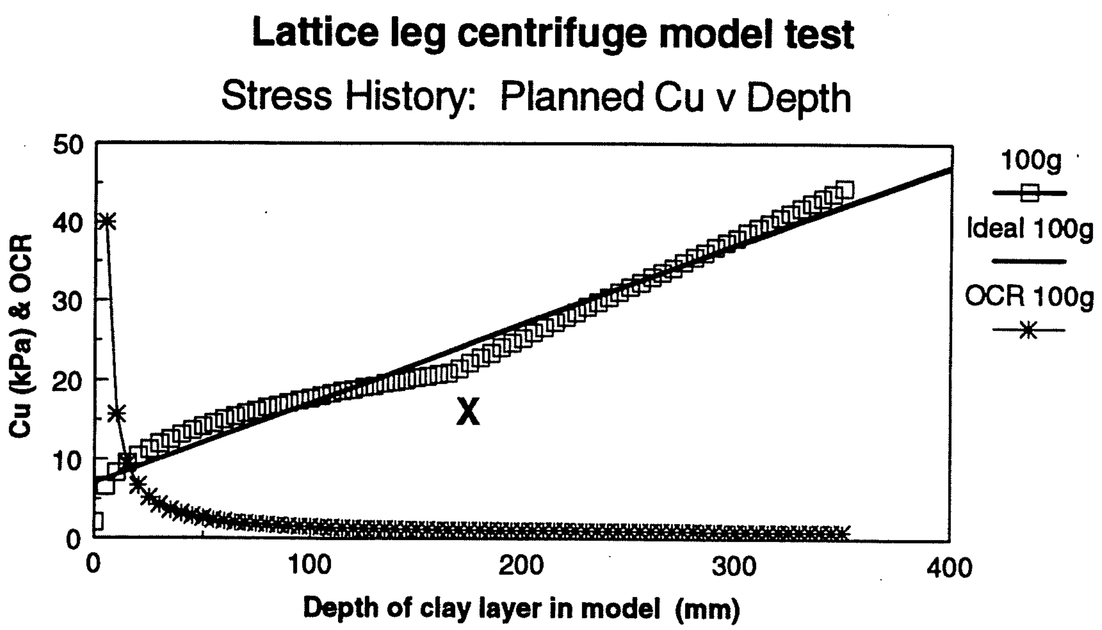

Figure 5 Variation of c_u and OCR with depth at 100 g (Springman, 1991)

Table 3a Properties of kaolin clays: frictional strength (Airey, 1984)

Clay	*Method of consolidation*	I_p %	ϕ_{txc}' (°) or ϕ_{psa}'	ϕ_{txe}' (°) or ϕ_{psp}'	*Source*
Kaolin	Isotropic, TX	20	24	24	Yong & McKyes (1971)
Kaolin	Isotropic, TX	25	29.2	36	Broms & Casbarian (1965)
Spestone kaolin	Isotropic, TX	32	22.6	20.5	Nadarajah (1973)
Spestone kaolin	K_o , TX	32	20.8	28.0	Nadarajah (1973)
Spestone kaolin	K_o , PS	32	20.9	21.7	Sketchley (1973)

Table 3b Properties of kaolin clays: undrained strength (Airey, 1984)

Clay	*Method of consolidation*	I_p %	$(c_u/\sigma_{vc}')_{txc}$ or $_{psa}$	$(c_u/\sigma_{vc}')_{txe}$ or $_{psp}$	*Source*
Kaolin	Isotropic, TX	25	0.43	0.34	Broms & Casbarian (1965)
Spestone kaolin	Isotropic, TX	32	0.215	0.205	Nadarajah (1973)
Spestone kaolin	K_o, TX	32	0.205	0.175	Nadarajah (1973)
Spestone kaolin	K_o, PS	32	0.20	0.16	Sketchley (1973)
Spestone kaolin	K_o, PS	32	0.30	0.18	Ladd *et al.* (1977)

Airey (1984) summarised (Tables 3) the properties of various forms of kaolin (and for other clays not included here) where ϕ_{txc}', ϕ_{txe}', ϕ_{psp}', ϕ_{psa}', refer to angles of shearing resistance at failure (otherwise generally described as ϕ_{crit}' at the critical state) for triaxial (TX) compression, extension and plane strain (PS) passive, active respectively. Since 1978, speswhite kaolin has been supplied for laboratory testing in place of spestone kaolin, and Mair (1979) commented that both clays exhibited similar soil properties. Results in simple shear, on *normally consolidated* speswhite kaolin (I_p = 32 %) at constant volume gave $\phi' = 21.8^{o}$ (Airey, 1984) and $c_u / \sigma_{vc}' = 0.18$, whereas Al Tabbaa (1984) found $\phi_{txc}' = 23^{o}$ when OCR = 2.

Consolidation

Consolidation time factor $T_v = c_v\, t / h^2$ where c_v is the coefficient of consolidation in a vertical direction, t is time and h is the length of the drainage path (i.e. for two way drainage, model depth = 2h).

For speswhite kaolin undergoing a virgin loading increment of σ_v = 43 - 86 kPa in the consolidometer, $c_v = 2.7\ 10^{-7}$ m²/s, vertical permeability $k_v = 3.\ 10^{-8}$ m/s (Springman, 1989: c.f. Figure 6a, ex Al Tabbaa, 1987). Consolidation data from preparation of other centrifuge test specimens (Table 4) is also plotted on Figure 6a, indicating whether the stresses are increasing or decreasing together with a guide to the OCR. The values appear to fall on the higher side of Al Tabbaa's data, which are marked by the symbol ◦.

Al Tabbaa (ibid) also quotes values of k_v and horizontal permeability k_h (obtained from independent falling head and consolidation tests) for speswhite kaolin with respect to void ratio e:

$$k_v = 0.5\ e^{3.25}\ 10^{-6} \quad \text{mm/s} \tag{3a}$$
$$k_h = 1.43\ e^{2.09}\ 10^{-6} \quad \text{mm/s} \tag{3b}$$

for normally and overconsolidated states with $0.98 < e < 2.2$, $37\% <$ moisture content $w < 84\%$, and where k_h is derived from consolidation results (Biot). However, in Table 4, the data given showed that the values of $k_{v\ pred}$ by Equation 3a was up to 3 times larger than those measured in the 1 g consolidometer for unloading increments and in quite good agreement for virgin consolidation.

If $c_v = 10^{-7}$ m²/s for unloading - reloading conditions, for a clay depth of 60 mm, then time for 90% consolidation, T_v = 0.848, and $t_{90} = 0.848 \times (0.06/2)^2/10^{-7} = 2.1$ hours; for a clay depth of 350 mm (e.g. stress history from Figures 4 and 5), $\sigma_v > 86$ kPa in the lower half of the model where the sample would be normally consolidated. If a conservative value of c_v was taken as $2.7\ 10^{-7}$ m²/s for a normally consolidated clay, then $t_{90} = 0.848 \times (0.35/2)^2 / 2.7\ 10^{-7} = 26.7$ hours.

Table 4 Consolidation data from centrifuge models in large 1 g consolidometer

Clay	σ_{vc}' *kPa*	*e*	c_v *mm²/s*	k_v 10^{-6} *mm/s*	$k_{v\ pred}$ 10^{-6} *mm/s* *Eqn 3a*	*Source*
Speswhite kaolin	256 - 450	-	0.3	0.72	-	Bransby (1993)
	450 - 120	1.21	0.57	0.34	0.9	
	450 - 60	-	0.58	0.35	-	
Speswhite kaolin	100 - 200	1.30	0.18	0.95	1.17	Ellis (1993)
Speswhite kaolin	54 - 91	1.54	0.25	2.87	2.03	Sharma (1993)
Speswhite kaolin	43 - 86	1.54	0.27	2.06	2.03	Springman (1989)

Therefore, for such deep samples, it is advisable to incorporate a thin sand layer across most of the clay layer at mid-depth to aid dissipation of pore pressures (Phillips, 1988). This sand layer would be linked to the drainage system at the top and bottom of the clay boundaries to facilitate drainage and reduce consolidation time by a factor of 4 (to less than 7 hours).

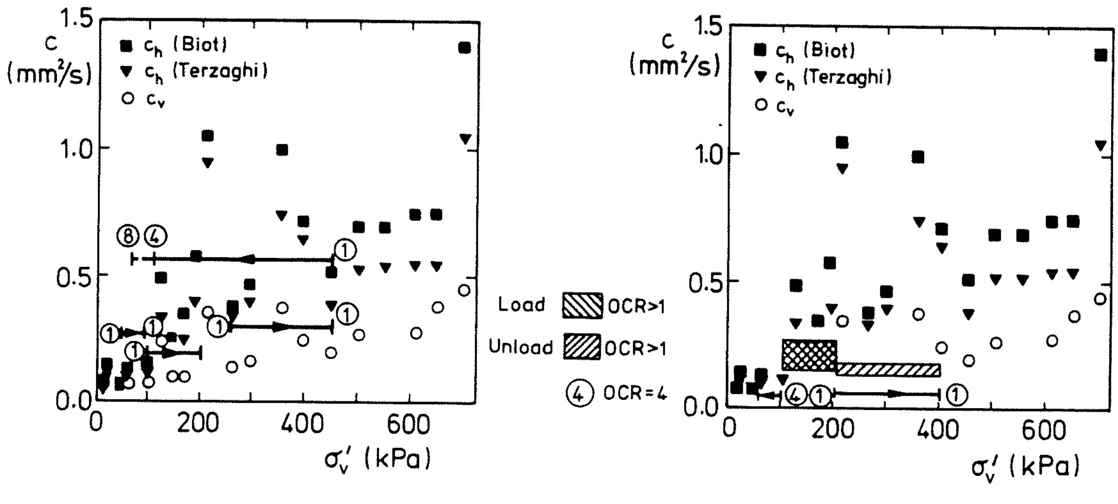

(a) centrifuge sample comparison

(b) KRF comparison

Figure 6 Variation of c_v for speswhite kaolin with σ_v' (Al Tabbaa, 1987)

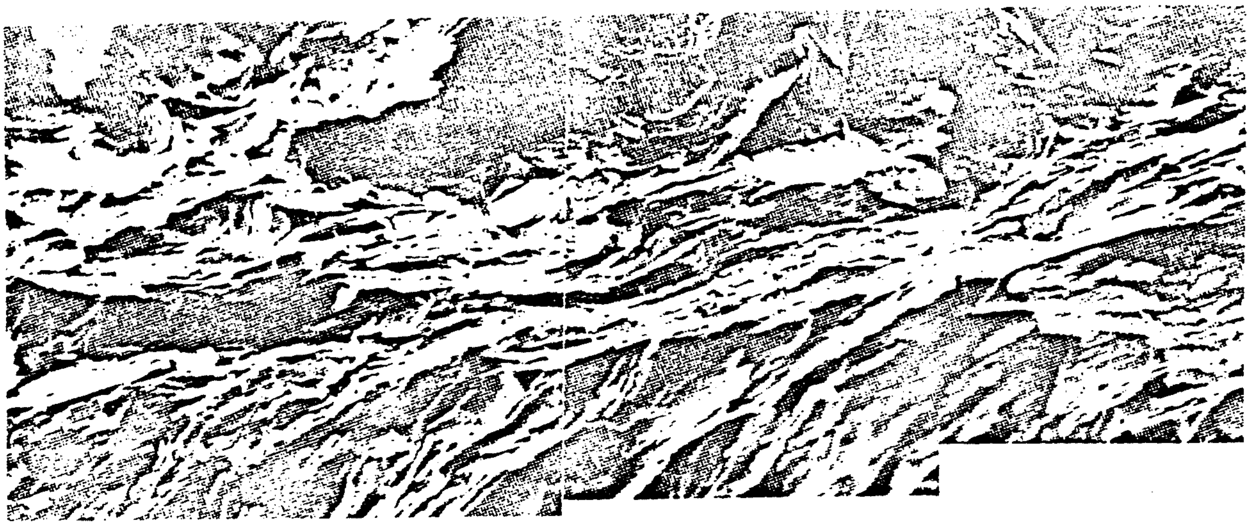

1 μm

(a) in kaolin (Tovey, 1970)

2 μm

20 μm

(b) in KRF (Mozuraitis and Springman, 1993)

Figure 7 Electron micrographs of shear surfaces

Properties of kaolin compared with kaolin mix soils

Sometimes it is necessary to increase the strength and stiffness of 'laboratory' soils with large clay fractions, and this may be achieved by adding granular material. Tovey (1970) and Lawrence (1980) discuss the tendency of high clay fraction soils to develop low strength residual shearing surfaces. Electron micrographs can show how the platey clay particles align themselves along polished planes with a residual angle of friction $\phi'_{res} < \phi'_{crit}$ (Figure 7a). The addition of silty/sandy particles prevents this drop in frictional shear strength along potential failure surfaces by reducing the % clay fraction below 65%. Figure 7b shows how the individual kaolin flakes of approximately 2 μm in particle size have clumped together in 'peds' with large voids in between. On consolidation, it is the voids between the 'peds' which are reduced to create a more closely packed soil. Micrographs taken of the shear surface at larger scale show no obvious shear plane, which might be anticipated to be of thickness about 10 μm.

Rossato *et al.* (1992) discuss the implications of mixing speswhite kaolin (denoted as K) with either silt and sand particles (KSS) or just sand (H-K) to prevent the formation of these slickensided surfaces at values of ϕ' below the critical state. They quote strength and stiffness results for low OCR , K_o consolidated samples and laboratory tests against plasticity index for comparison. Figures 8 and 9 summarise their findings. Classification test data (including liquid limit LL and plastic limit PL) and normalised undrained strength are given in Table 5a. Table 5b shows some critical state and frictional strength parameters, where λ is the slope of the isotropic normal compression line in specific volume, v - ln p' space (where p' is the mean effective stress), κ is the nominal slope of the unload-reload line in v - ln p' space, N is the intercept of the isotropic normal consolidation line at p' = 1 kPa.

A new mix was designed for use in Cambridge undergraduate experiments in the direct shear box, in which 70% speswhite kaolin was mixed with 30% 180 grade silica rock flour (KRF) under vacuum at approximately 80% moisture content. The slurry was one dimensionally consolidated to 200 kPa, before unloading, sampling, sealing and storage. On extrusion into the 100 mm square shear box apparatus, various consolidation routines were followed via σ'_{vc} = 400 kPa, to bring the deposit to an OCR of 1, 4 and 8. Shearing was carried out at approximately 0.06 mm/min by the undergraduates and also at a slower rate of 0.03 mm/min (Mozuraitis and Springman, 1993). Peak (ϕ'_{max}) and critical state (ϕ'_{crit}) shearing resistance is reported for each series in Table 5c. Whereas previous overconsolidated speswhite kaolin samples (OCR = 8) had peaked higher, but approached a much lower ultimate (residual) value of ϕ' than those for the OCR = 4 and normally consolidated samples. This series of tests on KRF showed that the overconsolidated (OCR = 8) sample exhibited a higher value of ϕ'_{crit} , although this was still falling slightly at an axial strain of 11 % (Table 5c). Boundary effects in the direct shear box become important at smaller strains than this, so further straining was not pursued.

Table 5a Properties of kaolin/kaolin mix clays: undrained strength

Clay	*Method of consolidation*	*Clay %< 2μm*	*LL %*	*PL %*	*I_p %*	*$(c_u/\sigma_{vc}')_{txc}$*	*$(c_u/\sigma_{vc}')_{txe}$*	*Source*
K	K_o , TX	82	63	33	30	0.197	0.18	Rossato *et al.* (1992)
KSS	K_o , TX	43	35.5	17	18.5	0.233	0.166	Rossato *et al.* (1992)
H-K	K_o , TX	6	-	-	2	0.32	0.06	Rossato *et al.* (1992)
KRF	K_o , TX	55-65	38	21	17	0.244	-	Wilkinson (1993)

Table 5b Properties of kaolin/kaolin mix clays: critical state and frictional strength

Clay	*Method of consolidation*	λ	κ	*N*	*ϕ_{txc}' (°)*	*ϕ_{txe}' (°)*	*Source*
K	K_o, TX/oedometer isotropic, TX	0.187 (mean)	0.028 (mean)	3.20 3.13	23 23	23 -	Al Tabbaa (1987)
KSS	K_o ,TX	0.086	0.019	3.13	24.1	26.9	Rossato *et al.* (1992)
KRF	K_o, isotropic TX	0.122	0.02	2.6	-	-	Wilkinson (1993)

Table 5c Properties of kaolin mix clays: direct shear tests on KRF

OCR	*K_o normal consolidation to σ_{vc}' (kPa)*	*ϕ_{max}' (°) at ε (%) $d\varepsilon/dt$ = 0.06 mm/min*	*ϕ_{crit}' (°) at ε (%) $d\varepsilon/dt$ = 0.06 mm/min*	*ϕ_{max}' (°) at ε (%) $d\varepsilon/dt$ = 0.03 mm/min*	*ϕ_{crit}' (°) at ε (%) $d\varepsilon/dt$ = 0.03 mm/min*
1	400	23	19	23.3 (5%)	20.6 (11%)
4	400	25	20	25.2 (1.2%)	19.1 (11%)
8	400	28	25	31.7 (1.5%)	24.1 (11%)

Subsequently, Wilkinson (1993) carried out classification tests and undrained triaxial compression tests on samples taken from the same batch (Tables 5a and 5b). The critical state line at failure for KRF is given in Figure 10a, together with the stress paths to failure in Figure 10b. The value of M indicated by the critical state line in Figure 10b is approximately 1.24, which suggests a value of ϕ' in excess of 30°. This is well above the expected value of M which should be about unity for $\phi_{crit}' = 25°$.

It can be seen from Figure 8 that the range of the particle size distribution for the KRF soil fell between that of the K and KSS mixes reported by Rossato *et al.*, (1992). The KRF sample was prepared by the Earth Sciences laboratory by disaggregating the particles using sodium hexametaphosphate, followed by agitation for about 4 hours and then sedimentation, with machine measurement and analysis according to Stokes' Law. The lower limit shown for KRF coincides with the theoretical distribution calculated from the quoted distribution of a 70% speswhite kaolin and 30% 180 grade silica rock flour and analysis for a specimen taken from the failure plane of the direct shear box under $\sigma_{vc}' = 50$ kPa, OCR = 8. The upper limit is that from the failure plane for a normally consolidated sample in the direct shear box under $\sigma_{vc}' = 400$ kPa, the curve for $\sigma_{vc}' = 100$ kPa, OCR = 4 falls just below the upper limit (all samples came from the same sampling tube and were sheared in tests by Mozuraitis. This tends to indicate that there may be some crushing of particles along the failure plane due to shearing under normal stresses greater than 50 kPa, although there has not yet been an opportunity to evaluate whether this apparent trend was due to a statistical variation or operator bias.

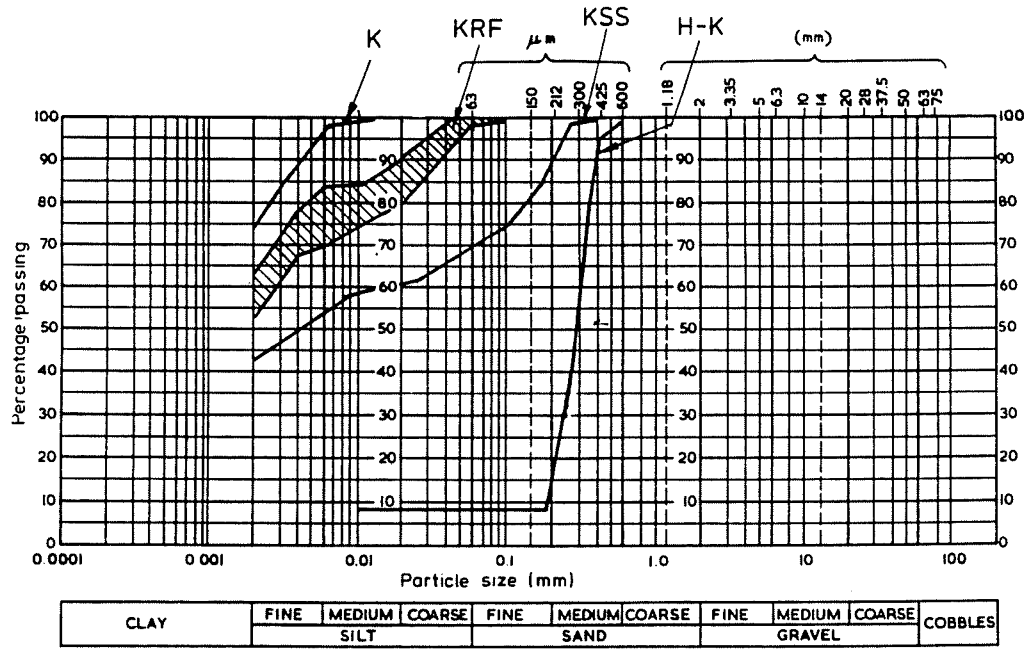

Figure 8 Particle size distribution for kaolin and kaolin mix soils (after Rossato *et al.*, 1992; Mozuraitis and Springman, 1993).

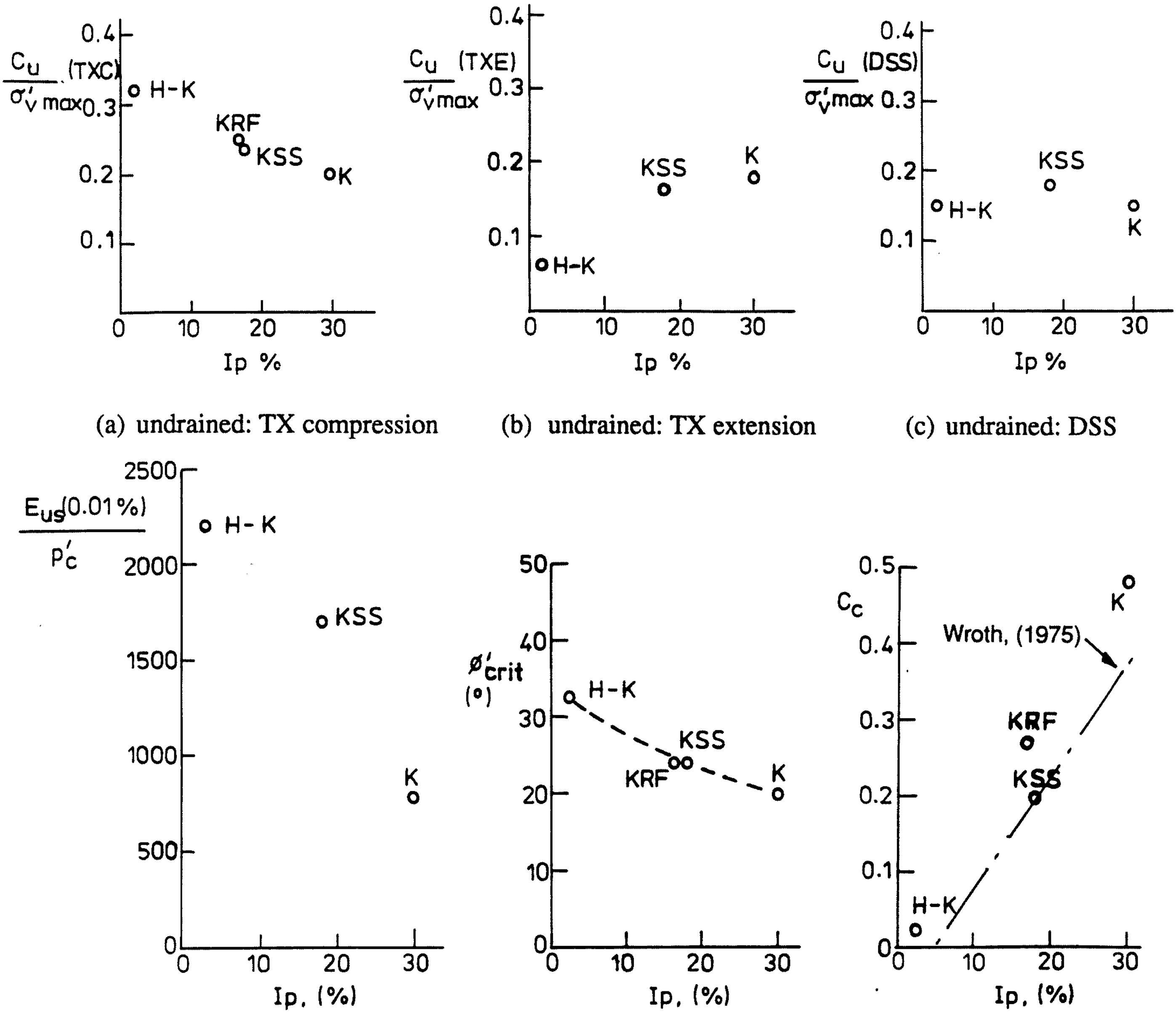

(a) undrained: TX compression (b) undrained: TX extension (c) undrained: DSS

(d) secant stiffness (e) frictional: critical state (f) compressibility ($e - \log_{10}\sigma_v'$)

Figure 9 Strength and stiffness parameters v I_p for kaolin and kaolin mix soils (Rossato *et al.*, 1992; Wilkinson, 1993; Mozuraitis and Springman, 1993)

The KRF mix appears to be more compressible than the trend line (Wroth, 1975) shown for kaolin based soils implies (Figure 9f). However, there is closer agreement for the values of ϕ_{crit}' (although the KRF value is derived from a direct shear box test (not direct simple shear, DSS), and the others from TXC; Figure 9e), and also for the $c_u/\sigma_{v\,max}'$ for triaxial compression (Figure 9a) where $\sigma_{v\,max}'$ is the maximum vertical effective stress experienced by the triaxial specimen.

These kaolin mixes were found to be 3 - 10 times more permeable than kaolin (Table 4) under similar OCRs and σ_v'. This is a significant advantage in relation to centrifuge modelling, because it allows the time needed for model preparation to be reduced.

Comparisons between the data of normalised undrained strength $c_u / \sigma_{v\ max}'$ in triaxial extension (Figure 9b) or direct simple shear (Figure 9c) and equivalent values for the KRF soil, and also of undrained secant modulus E_{us} at 0.01% axial strain for pre-shear mean effective normal consolidation stress p_c' (Figure 9d) will be done when the Cambridge triaxial apparatus is fitted with a small strain measuring device. Wilkinson's (1993) triaxial compression tests gave E_{us} at 1% axial strain of 7 MPa for a range of p_c' = 100 - 200 kPa.

The general conclusions to be drawn are that both the KSS and KRF mixes approximate the behaviour of natural soils (e.g. Glacial tills) rather more closely than the pure speswhite kaolin. Undrained and frictional strength in compression and stiffness are higher and more comparable to 'real' soils. The trend (Figure 9a) also shows decreasing strength with increasing plasticity, whereas the strength in extension and shear increases slightly. The deformation mechanisms exhibited by any marine structure will depend on the response of the soil to the loading regime. This is influenced greatly by the recent stress path, the magnitude of stiffness following load reversal and the strength due to compression, extension or shear, so it is appropriate to be able to model this behaviour. Any tendency to form residual shear surfaces in a model at lower values of ϕ' than expected in the field will also affect the load transfer that must occur when soil reaches the peak 'brittle' strength which has been associated with interlocking, as it softens towards the critical state and then to a residual value. The graphs given in Figure 9 can be used to design appropriate mixes to suit these specific field conditions.

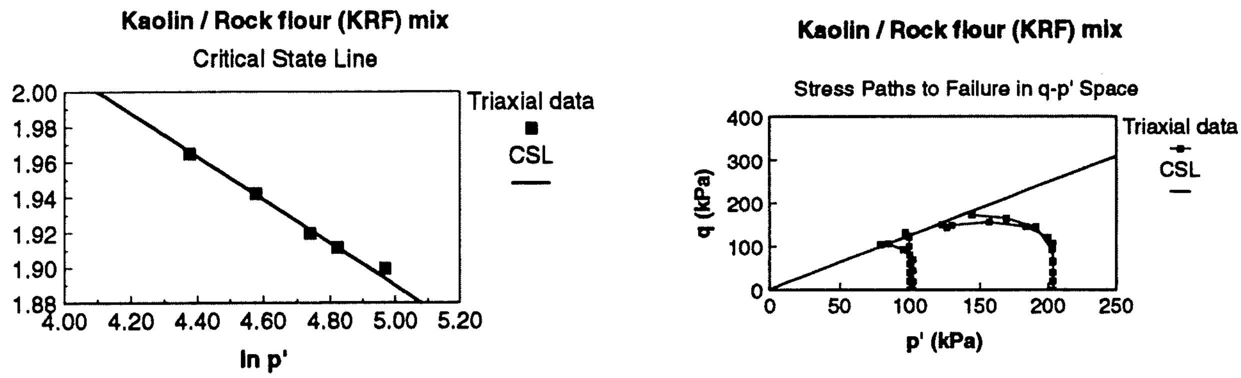

(a) critical state line

(b) stress paths

Figure 10 Critical states for KRF (Wilkinson, 1993)

Wilkinson's (1993) data fall close to a straight line for v - ln p' space in Figure 10a, with λ = 0.122. The stress paths to failure (Figure 10b) show that the final positions reported by Wilkinson appear to exhibit some additional strength due to interlocking.

Laboratory model preparation

Mixing, placement, consolidation

For centrifuge models made in the laboratory using reconstituted soils, it is generally necessary to mix the powder into a slurry under a vacuum for a period not less than 2 hours to ensure that it will be homogeneous and fully saturated. The slurry may then be placed inside the liner/consolidometer or strongbox ensuring that no air bubbles are included. Porous strips (e.g. 3 mm 'Vyon' porous sintered plastic) and filter papers, saturated with de-ionised water will be located above and below the sample as required. The consolidation pressures will be applied using gas pressure behind the piston of a cylindrical jack. This bears on a rigid plate which is in contact with the drainage layers on top of the soil deposit. The gas pressure may be regulated to produce the required total stress on the consolidating deposit.

In order to minimise the likelihood of cavitation occurring due to suctions caused by unloading from the maximum consolidations stress, σ_{vc}', this should be carried out in increments of stress less than 100 kPa with all drains open, allowing for equilibration of the pore pressures at each stage. Possible air entry at the edges of the model is limited by permitting controlled swelling.

Critical State Soil Mechanics properties may be used to estimate the amount of compression expected from a speswhite kaolin slurry at a nominal 120% moisture content to equilibrium under the consolidating load. For fully saturated speswhite kaolin, with specific gravity G_s = 2.61 (Airey, 1984), initial void ratio:

$$e = v - 1 = w\,G_s = 1.2 \times 2.61 = 3.132$$

This moisture content is roughly 40% greater than the equivalent value of $e = 2.13 \pm 0.03$ quoted by Al Tabbaa (1987) at $p' = 1$ kPa for one dimensional consolidation in a 100 mm diameter oedometer. One dimensional compression index, λ was found by several researchers at Cambridge to be non-linear, and to be within $0.25 < \lambda < 0.31$ for $50 < \sigma_{vc}' < 80$ kPa. A typical range is quoted by Airey (1984) with λ decreasing from 0.38 at $\sigma_{vc}' = 25$ kPa to 0.21 at $\sigma_{vc}' = 250$ kPa.

Airey (1984) and Al Tabbaa (1984) noted from independent test series that earth pressure coefficient at rest for normally consolidated soil, $K_{o\,nc}$ = 0.69. A commonly used approximation is:

$$K_{o\,nc} = 1 - \sin \phi_{crit}' \qquad (4)$$

which for critical state values, $20^o < \phi_{crit}' < 23^o$ gives $0.66 > K_{o\,nc} > 0.61$, which is lower than the laboratory values. Bolton (1991) suggests using a mobilised angle of shearing at rest ϕ_o':

$$\phi_o' = \phi_{max}' - 11.5^o \tag{5}$$

as a function of the peak angle of shearing ϕ_{max}' ($\phi_{max}' = \phi_{crit}'$ when there is no dilation). If this ϕ_o' is substituted into the expression for active earth pressure coefficient, $K_o = 0.7$ when $\phi_{max}' = 21.5^o$ and $\phi_o' = 10^o$. This agrees far better with experimental data.

After consolidation of the model offshore soil in the jack up 'lattice leg' centrifuge model test, when $\sigma_{vc}' = 110$ kPa (Springman, 1991), moisture content samples showed $w = 56$ %, and so $e = 2.61 \times 0.56 = 1.462$. If $\sigma_h' = K_{o\,nc}\,\sigma_{vc}'$, and $K_{o\,nc} = 0.69$, mean effective stress $p' = (\sigma_{vc}' + 2\sigma_h')/3 = 0.793\,\sigma_{vc}' = 87.3$ kPa. The expression relating void ratio to mean effective stress:

$$e = e_o - \lambda \ln (p'/p_o') \tag{6}$$

implies that if the slurry has $e_o = 3.132$ at values of p_o' near to zero, e.g. $p_o' = 0.1$ kPa, $\lambda = 0.25$. This compares well with other large scale consolidation histories for speswhite kaolin in which $\sigma_v' = 86$ kPa, $w = 60$ % (Springman, 1989) and so $\lambda = 0.24$. Since the height of the sample is directly proportional to $1 + e$, the initial volume (and height) of clay slurry may be determined.

For the consolidation and stress history given in Figure 4, a reduction in height to just less than 50 % of the original slurry was allowed for to ensure that there was sufficient depth of clay following consolidation to trim the sample as required.

Table 6 Soil/perspex friction characteristics (Waggett, 1989)

Interface	*Lubricant*	*OCR*	*adhesion, δ °*
kaolin/kaolin	Nil	1	18.8
"	"	8	28.3
kaolin/perspex	Nil	1	11.9
"	"	8	18.8
"	Adsil spray	1	6.3
"	"	8	14.0
"	Silicone grease	1	2.3
"	"	8	5.1

An important aspect of the use of plane-strain strongboxes is the assumption that they will indeed ensure plane strain conditions during consolidation, e.g. for a 850 mm diameter tub, that the vertical consolidation settlement will be uniform, that there will be no significant lateral strain, and for the 200 mm wide by 675 mm long plane strain package with a perspex front window, that there will be no significant side friction acting on the soil model. Lubricants are applied to the walls of these strongboxes, which have been coated with low friction paint. Waggett (1989) conducted shear box experiments to give the residual friction on interfaces between kaolin and perspex, as treated by various lubricants (Table 6).

For both overconsolidation ratios investigated, friction was least using silicone grease, giving the closest approximation to the assumption that the principal stresses at the boundary of the model are vertical and horizontal. However, silicone grease is not transparent. Where side visibility is required, Adsil lubricant (or an equivalent, e.g. Ambersil) can be adopted for the boundary between perspex and kaolin.

Instrumentation

Common types of instrumentation inserted in a clay matrix are:

* pore pressure transducers,
* for contamination problems, resistivity probes (Hensley, 1989; Hellawell, 1993)
* for dynamic applications (e.g. earthquake studies), accelerometers (Kutter, 1982).

Druck pore pressure transducers (PPTs) are capable of measuring various magnitudes of pore pressures, and typically, the 350 kPa range are used. They are cylindrical in shape, 6.4 mm in external diameter, with a main body 13 mm long. They should be inserted prior to the addition of the final loading increment in the consolidometer, having unloaded the clay, in stages of 100 kPa or less, to zero excess load at 1 g.

Any subsequent consolidation settlement or swelling should be allowed for in planning the installation depth of these PPTs. The holes obtained following insertion of the PPTs are backfilled with slurry, which is injected through a syringe to ensure that any air will be excluded from the soil matrix. The transducer wires are taken out through special ports in the side of the 850 mm diameter tubular strongboxes or pressed into the rear of the plane strain soil sample with the wires passing through a small slot in the piston.

Kutter *et al.* (1988) have discussed the implications of placing a large 'boulder' within the clay matrix based on a parametric finite element analysis. The relative stiffnesses of soil and diaphragm, permeability of the soil, types of loading and the orientation of the transducer were investigated, and it was found that the pore pressures obtained were over 100% greater than expected for a 15 kPa stress increment for PPTs installed in very soft soils, with a modulus $E = 1000$ kPa, and 10% greater for $E = 10000$ kPa. The possible reinforcing effect of the transducers and their cables must be considered when planning their installation, and in subsequent back analysis of test data.

In future apparatus developments, PPTs may be made in the form of miniscule chips, interrogated by a remote trigger. By this means, it is hoped that the difference in the measured and the true pore pressure (that would have existed in the soil in the absence of the PPT) due to interference between the soil, the instrumentation cabling and transducer will be reduced significantly. In the meantime, care is necessary when designing and installing PPT layouts.

Stress paths

Consolidation

If it is assumed that one dimensional consolidation occurs from a slurry at minimum stress up to the maximum consolidation pressure (point A; Figure 11), with the major and minor principal stresses vertical and horizontal respectively, then for a constant K_o value, the effective stress path in q - p' space would be OA. The gradient of this line is η_{knc}. A yield surface of some shape passes through point A. If we assume that the soil may be modelled by Critical State theory (Schofield, 1980; Muir Wood, 1990), the yield locus (OAX) for any value of $\eta = q / p'$ will be described by the following equation:

$$\eta / M = \ln (p_{oi}' / p') \qquad (7)$$

where $(0, p_{oi}')$ is point X on the isotropic consolidation line in q - p' space, and M is the Critical State parameter. The Critical State Line (CSL) is described by the relationship:

$$q = M p' \qquad (8)$$

where:

$$M = 6 \sin\phi_{txc} / (3 - \sin\phi_{txc})$$
$$M = -6 \sin\phi_{txe} / (3 + \sin\phi_{txe})$$

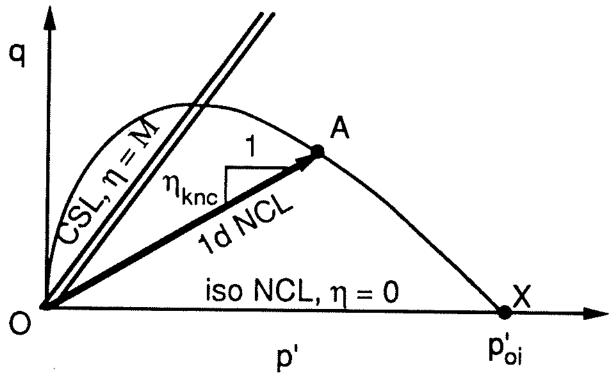

Figure 11 Effective stress path in q - p' space

The active and passive limits may also be drawn for vertical and horizontal principal stresses since:

$$q = |\sigma_v' - \sigma_h'| \qquad\qquad p' = (\sigma_v' + 2\sigma_h')/3$$

for $\sigma_v' > \sigma_h'$; $\sigma_h' = K_a \sigma_v'$ where: $K_a = (1 - \sin\phi_{crit}')/(1 + \sin\phi_{crit}')$ (9)

for $\sigma_v' < \sigma_h'$; $\sigma_h' = K_p \sigma_v'$ where: $K_p = (1 + \sin\phi_{crit}')/(1 - \sin\phi_{crit}')$ (10)

Similarly, we can determine the volumetric behaviour by considering the v - ln p' space, where v is specific volume (Figure 12). The isotropic normal compression line (iso NCL) has $\eta = 0$, and a one dimensional compression line, with $M > \eta_{knc} > 0$, plotting parallel to and between the iso NCL and the CSL. The implication for any point A is that its position in v - ln p' space is identical to having been isotropically compressed to point X along the iso NCL and unloaded along an 'elastic' unloading-reloading (URL) κ line to point A, but that there is also a significant component of deviator stress q (Point A; Figure 11).

A difficulty with the model described above is that it predicts $K = K_o = 1$. Instead of using this model, Bolton's ϕ_o' (Equation 5) may be substituted into Equation 9 instead of ϕ_{crit}' to determine one dimensional virgin compression $K_{o\,nc}$ for the stress path OA (Figure 13).

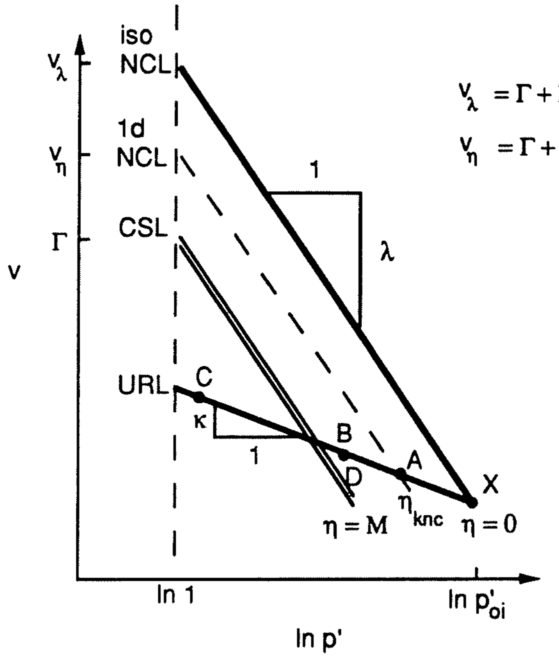

Figure 12 v - ln p' space

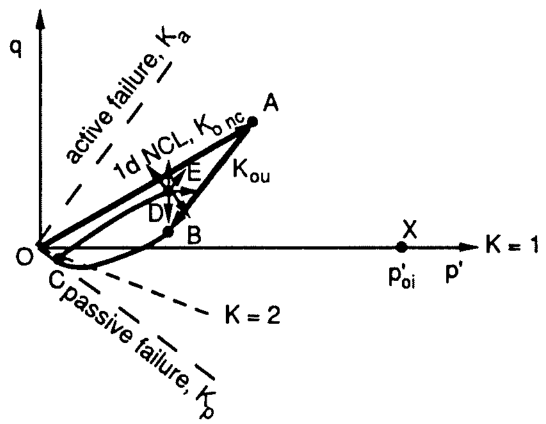

Figure 13 Stress path: slurry, consolidation, unloading and reloading in the centrifuge

Model making

On unloading from the yield surface, during the subsequent stages of the model making, there would be some reduction in effective stress unless the clay is capable of retaining a considerable suction. Pore suctions of up to 30 kPa have been measured in kaolin just prior to the centrifuge flight, when supplies of water to the top and bottom drains had been cut-off and air entry to the clay was limited.

In reality, it is difficult to maintain suctions in a relatively permeable clay such as kaolin, and so the effective stress reduces, following a path ABC, and the value of the earth pressure coefficient changes accordingly, as the stress path moves towards the passive failure line (Figure 13). Various empirical estimates may be used to determine the earth pressure coefficient on unloading, K_{ou}.

Al Tabbaa (1987) and Muir Wood (1990) recommend Wroth's (1975) expression, but for a smaller range of OCR =< 2, so that this is acceptable for path AB:

$$K_{ou} = OCR\ K_{o\,nc} - \{(OCR - 1)\,\nu' / (1 - \nu')\} \qquad (11)$$

where $OCR = \sigma_{v\,max}' / \sigma_v'$ and ν' is the drained Poisson's ratio. This assumes that the soil behaves elastically and isotropically immediately following unloading, along a straight κ line in q - p' space. For greater OCRs, the path BC is observed to curve, and various researchers recommend:

$$OCR = \{K_{ou} / K_{o\,nc}\}^{1/\alpha} \qquad (12)$$

with $\alpha = 0.5$ (Muir Wood, 1990) or 0.464 (Al Tabbaa, 1987) or $\alpha = 1.2 \sin \phi_{crit}'$ (Schmidt, 1966), which for kaolin with $\phi_{crit}' = 21.5^\circ$ gives $\alpha = 0.44$. Wroth's (1972) expression (Equation 13) is dependent on the index properties of the clay and was said to be valid for all OCRs (Al Tabbaa, 1987):

$$m = 0.022895\, I_p + 1.22$$

where I_p is in % , so that $m = 1.95$ for speswhite kaolin and:

$$m[\{3(1 - K_{o\,nc})/(1 + 2K_{o\,nc})\} - \{3(1 - K_{ou})/(1 + 2K_{ou})\}] = \ln\{OCR(1 + 2K_{o\,nc})/(1 + 2K_{ou})\} \qquad (13)$$

If drained unloading is continued until the soil is in a state of incipient passive failure, when the horizontal effective stresses are K_p times the effective vertical stress, then the stress path will tend to become tangential to the limiting line for passive failure at C.

Centrifuge flight

As the centrifuge rotates faster, the self weight of the soil is increased with accelerating gravity field, and the pore pressures will respond immediately. Usually this is of the order expected for a fully saturated clay, and the total stress change causes an increase in pore pressure equal to the increment of self weight. Once consolidation has been permitted, the effective stress path will tend to approach the $K_{o\ nc}$ line (path OA; Figure 13) until the clay is in equilibrium with the stresses imposed by the centrifuge gravity field (path CD; Figure 13). The earth pressure coefficient during reloading K_{or} for speswhite kaolin may be approximated by either of two expressions, the first after Mayne and Kulhawy (1982):

$$K_{or} = K_{onc} [\, OCR / (OCR_{max})^{1-\alpha} - 0.75 \{(OCR / OCR_{max}) - 1\}] \qquad (14)$$

where OCR_{max} occurs at point C in Figure 13. The second expression is after Schmidt (1983):

$$K_{or} = K_{onc} [1 + \{(OCR_{max}{}^{\alpha} - 1) / (OCR_{max} - 1)\} \{OCR - 1\}] \qquad (15)$$

Finally, the subsequent behaviour of the clay deposit due to any perturbation DE (Figure 13) will depend on the recent strain path (Path 1; Figure 14) and the direction of the loading increment (Path 2; Figure 14). For overconsolidated swelling layers directly underneath a vertical load, the direction of the strain path will be reversed, leading to a stiff response, (LHS; Figure 14) whereas the section adjacent to the load will undergo continuing 'extension' which will be 'soft' (RHS; Figure 14). This situation is reversed for a normally consolidated deposit which is gradually accreting sedimentary layers.

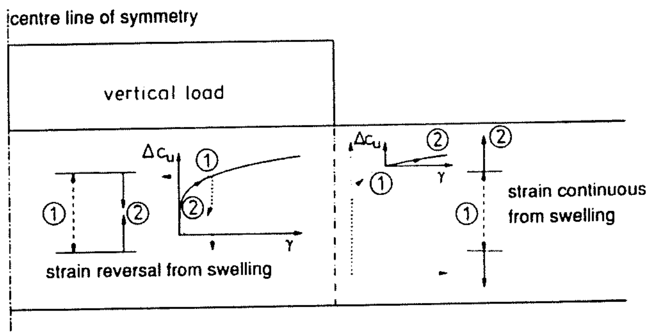

Figure 14 Strain directions under a vertical load (swelling overconsolidated clay; after Sun, 1989)

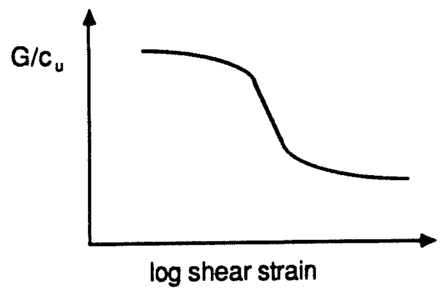

Figure 15 G/c_u as a f(shear strain)

Measurement of stiffness and strength

If centrifuge model tests are to be used to calibrate numerical analysis, determination of stiffness and strength is essential. The usual caveats which allow these characteristics to be derived from in-situ tests are relevant (Meigh, 1987), but further thought is necessary when applying any empirical rules at small scale. To date, miniature vane shear testing apparatus, penetrometers and piezocones have been developed, and are in use worldwide (Bolton *et al.*, 1993; Corte *et al.*, 1991). Stewart and Randolph (1991) designed a bar penetrometer which shows promise for calculating the undrained shear strength of deep soft clay layers.

Stiffness depends on a variety of factors including the magnitude of strain following the most recent load reversal. It is common that shear modulus G is related to c_u and shear strain γ in some empirical fashion (Figure 15) via laboratory tests. However, the direct measurement of stiffness is not yet possible in the centrifuge. In future, the incorporation of bender elements into the design of liners, in a similar fashion to that used in triaxial cells by Tang (1993), may permit the estimation of average small strain values of secant moduli E and G.

Vane shear testing

In the field, it is known (Mahmoud 1988) that for a homogeneous clay, c_u measured by the vane apparatus varies according to the vane aspect ratio and the rotation rate of the vane. In the centrifuge the length of the vane, L should be reduced with respect to the diameter, D so that:

* c_u is averaged over a smaller depth,
* a greater emphasis will be placed on c_u in the horizontal plane c.f. c_u (vertical)
* it is possible to conduct more vane tests over the depth of the clay layer (at least 1 vane depth should be left untested between each shearing)
* the effect of the shaft diameter:vane diameter is reduced (relative shaft/vane resistance and soil displacement due to insertion).

The vane aspect ratio (height/diameter) is usually of the order of 0.77 in the centrifuge, compared with 2 in the field (130 mm long, 65 mm diameter). For a test at 100g, a model vane (Figure 16a) 14 mm long and 18 mm diameter scales up to a prototype vane 1.4 m long and 1.8 m in diameter. The vane device is fitted with a 15° slip coupling which allows the component of friction on the pre-greased shaft to be separated from that due to the shear around the vane (Figure 16b). Centrifuge data (Cheah, 1981) showed that very similar profiles of c_u were obtained for model test vanes of aspect ratios of 1.5 and 0.77, but for a ratio of less than 0.5, a reduction in measured strength of more than 30% was observed.

At extremely fast rotation rates, viscous effects would cause the measured c_u to increase. At very slow speeds, significant consolidation occurs, again causing higher values of c_u. The optimal rotation speed is that which gives the lowest value of c_u, and this has been found in full scale practice as 6 °/min (Mahmoud, 1988).

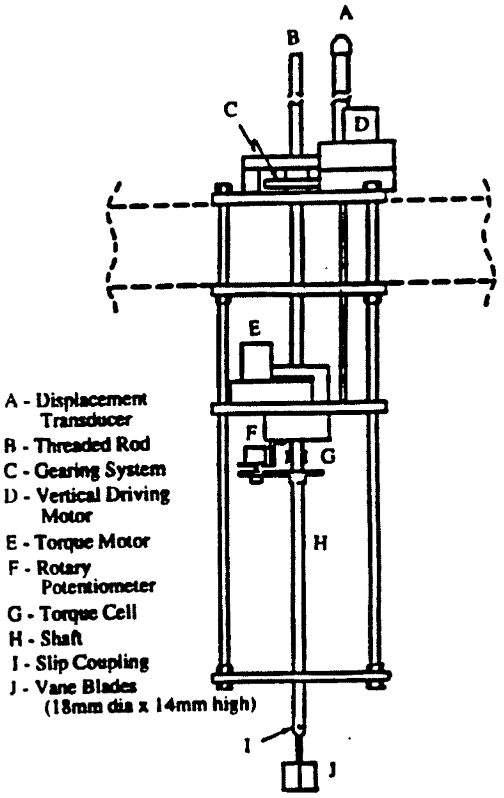

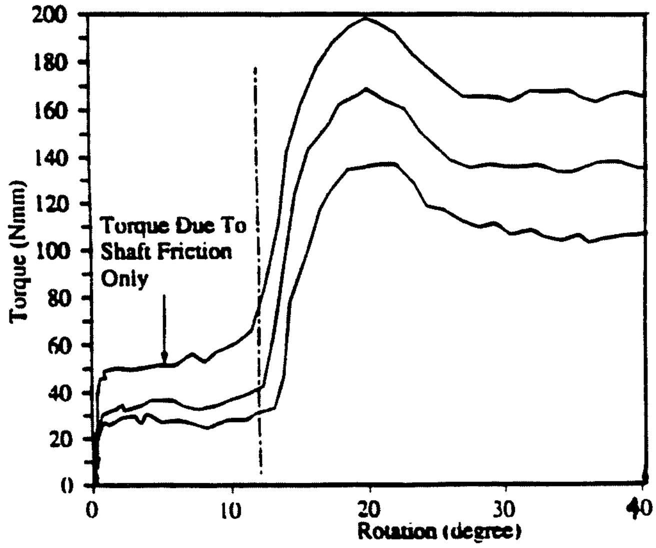

(b) typical test data (after Bolton *et al.*, 1993)

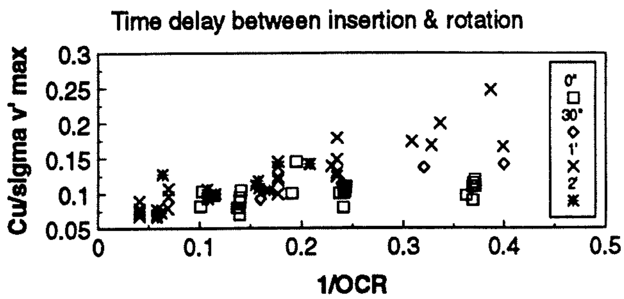

(a) apparatus (after Almeida, 1984)

(c) effect of time delay: insertion/rotation

Figure 16 Shear vane testing in the centrifuge

The testing procedures need to be carefully considered in view of the difference in scaling with respect to time. For example, the time relative to the strain rate, engendered by the shear vane will be identical in both cases, whereas the time taken for dissipation of the pore pressures following insertion of the vane will be affected by diffusion, which scales as n^2 faster. The centrifuge vane is expected to give higher strengths because there will be greater drainage, but reduced viscosity effects because the relative rotation rate is slower. In the centrifuge, the rotation rate which gave the lowest values of c_u for the 14 x 18 mm vane was 72 °/min (Almeida, 1984). This compares well with Blight's (1968) suggestion that for undrained rotation (degree of consolidation less than 10%), time factor T_v should be < 0.02 to 0.04, where t_f is time to failure:

$$T_v = c_v \, t_f / D^2$$

For a c_v of 0.27 mm²/s, and $D = 18$ mm, then $t_f < 25$ s, which at a rate of 72 °/min is roughly 30° rotation. It is usual that after the 15° rotation due to the slip coupling is discounted that the peak strength will be generated within a further 10° of rotation (Figure 16b).

The relationships between c_u, σ_v' and OCR used in design of the clay sample are based on the centrifuge vane data. At Cambridge, the vane is driven into the clay at between 2 and 6 mm/min, and on reaching the test depth, a rotary motor is engaged, and shearing is begun at 100 g after 1 minute. In the field, this delay is usually 5 minutes (equivalent to 5 x 60 / (relative diameter ratio)^2 = 23 seconds for radial drainage at the vane circumference at 100g), so the clay in the centrifuge model will have consolidated more, and higher strengths would be anticipated.

It is possible to analyse the torque T, applied at the failure on a cylindrical surface of diameter D, and height, L in terms of a peak and a residual value of c_u, depending on the assumptions made about the change of c_u with depth. If c_u increases linearly with depth, then it is usually considered acceptable to quote c_u at the vane mid-depth as the average value, determined by:

$$T = \pi c_u (D^3 + 3D^2 L) / 6 = \pi c_u D^3 / 0.55 \qquad (17)$$

Figure 16c shows the vane data from Figure 2c replotted with symbols describing the varying time delays between insertion and rotation. Additional time is required for rotation of the slip coupling, and this is usually between 15-30 s. Increasing time delay leads to greater measured strength, as might be expected. Further investigation is advisable, leading to standardised techniques and procedures over a range of gravity levels.

Figure 17a compares the variation of c_u (or s_u) determined by major laboratory tests on normally consolidated clays against vane shear test data corrected for strain rate (Bjerrum, 1973). Figure 17b shows the profile of c_u deduced from in-flight vane tests at 100 g, (uncorrected by Bjerrum's factor μ), for the jack up 'lattice leg' sample referred to in Figures 4 and 5, compared with the design values which were also based on vane shear tests. A reasonable approximation has been achieved for the peak shear strength over the top 200 mm of the kaolin, assuming that the average c_u represents the shear strength at the mid-depth of the vane. If this was translated to equivalent undrained strengths in triaxial compression or extension, then the trends shown in Figure 17a would indicate that the triaxial strength in compression is roughly 50% greater than the corrected vane strength, whereas the triaxial strength in extension is 50% smaller for $I_p = 32\%$.

Figure 17c compares an undrained strength ratio c_u / σ_{vo}' (or s_u / σ_{vo}') for a specific laboratory test normalised by the same ratio for a consolidated isotropic undrained triaxial compression (CIUC) test, plotted against ϕ'_{txc} (Kulhawy and Mayne, 1992), where σ_{vo}' is the current effective overburden stress. The CIUC test appears to give the greatest c_u for a range of ϕ_{txc}' relevant for clays. The values in compression are roughly double those in extension.

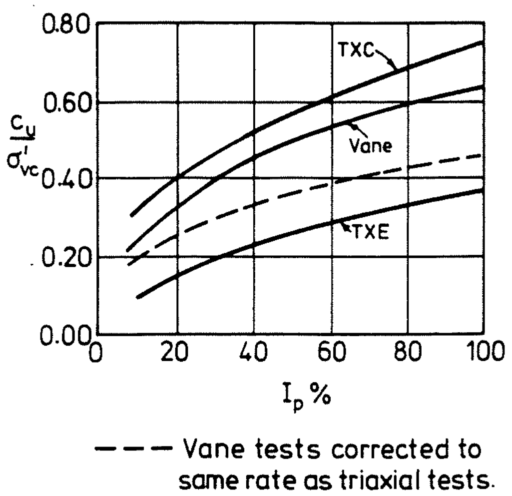

(a) Laboratory and field tests (Bjerrum, 1973)

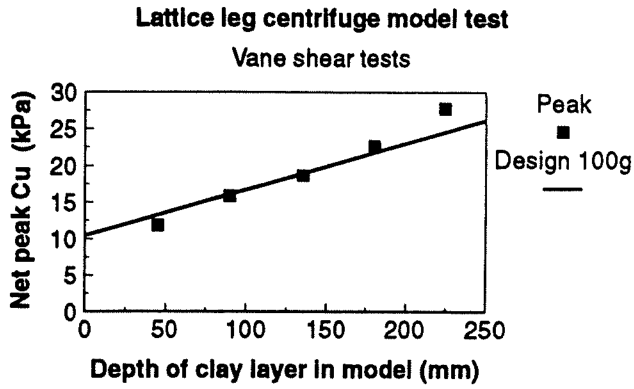

(b) Design and deduced values of c_u (Springman, 1991)

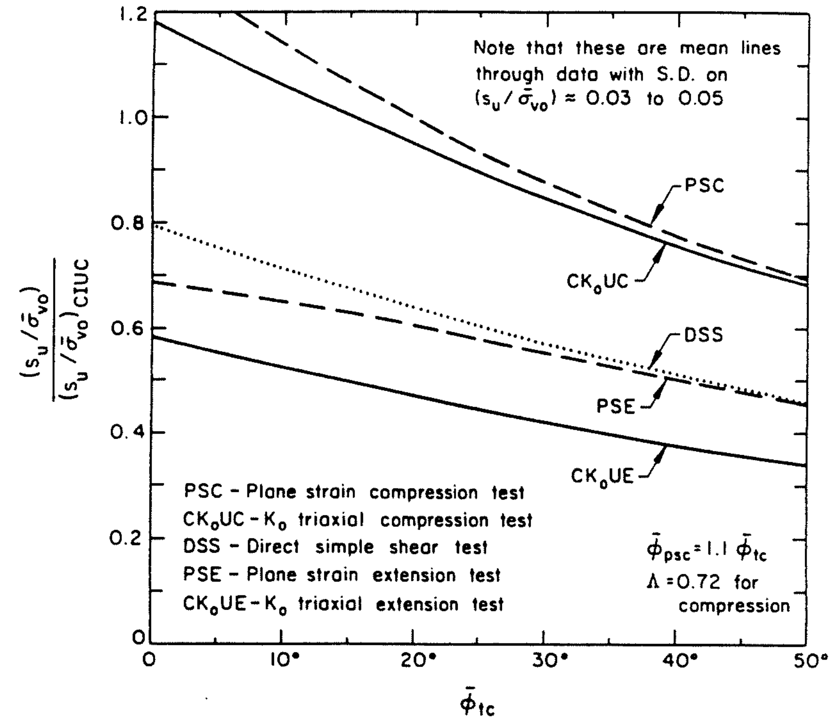

(c) Mean normalised strength ratios for laboratory tests (Kulhawy and Mayne, 1990)

Figure 17 Relationship between values of c_u (s_u)

Cone penetration testing

The cone penetrometer (Figure 18) presents different modelling difficulties although it has some advantages over the vane in that tests are quicker to perform and a continuous profile of soil resistance is obtained. Reproducing a 100 mm diameter field cone at 100 g implies a probe of 1 mm diameter! Clearly the slenderness ratio of such a device would be unacceptable, even before problems entailed in manufacturing and strain gauging a load cell had been considered.

Currently, the operational and cone design standards are being reviewed by a group of European Universities under an EC contract (Phillips & Gui, 1992). Recommendations will be made in due course, however it is Cambridge practice to use a standard cone of diameter 10 or 20 mm (Figure 18a), with a load cell located behind the tip or a piezocone (Almeida, 1984; Figure 18b) of 12.7 mm diameter, with a porous sintered stone at the tip of a 60° cone, and a rosette load cell located at the top of the shaft, but isolated from the friction exerted on the shaft. In a process similar to that experienced by the vane, faster insertion rates are likely to be subject to viscous effects, whereas slow penetrations will allow significant dissipation of pore pressures. Penetration rates of between 3 and 26 mm/s have been investigated in clay, and these are thought to fall in the intermediate range, with less than 13% difference in q_c (Bolton *et al.*, 1993) where q_c is the tip resistance.

An empirical relationship is used to estimate soil strength from a field cone factor N_c which is known to vary with OCR, ϕ_{crit}', pore pressure acting on the shoulder of the cone, and location of any pore pressure measurement devices (Mayne, 1992) where:

$$N_c = (q_c - \sigma_v) / c_u \qquad (18)$$

Full scale empiricism converted to model scale prediction leads to some uncertainty. Unlike in the field, the content of most centrifuge models is generally known, so these penetration tests are used mainly to check consistency of each test sample and to compare with in-flight vane test data.

Almeida (1984) discusses a pore pressure area correction ratio which can reduce the measured tip resistance by up to 50%. Springman (1989) found that the excess pore pressures generated when penetrating a soft clay layer of 10 kPa < c_u < 20 kPa at between 2 - 10 mm/s were significant. Minimal tip resistance was recorded using the piezocone shown in Figure 18b.

It is worth noting that there are some dimensional limitations on the performance of the penetrometer and that the apparatus should not be used closer than 5 d (5 cone diameters) from the location of another important section of the model or from the edge of the strongbox. Similarly, it is postulated that the proximity of the base of the strongbox or a stiffer founding stratum will increase the measured load for between 5 - 10 d above that boundary. These limitations were proposed by Phillips and Valsangkar (1987) for granular deposits. The interactions may be less noticeable in soft clays.

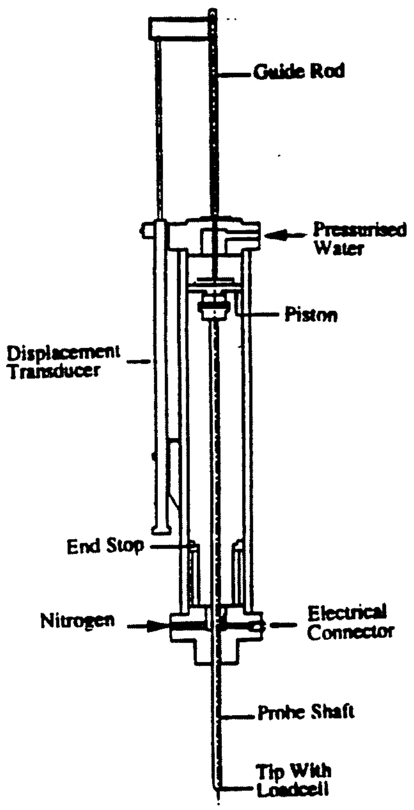

Figure 18a Cone penetrometer
(Phillips and Gui, 1992)

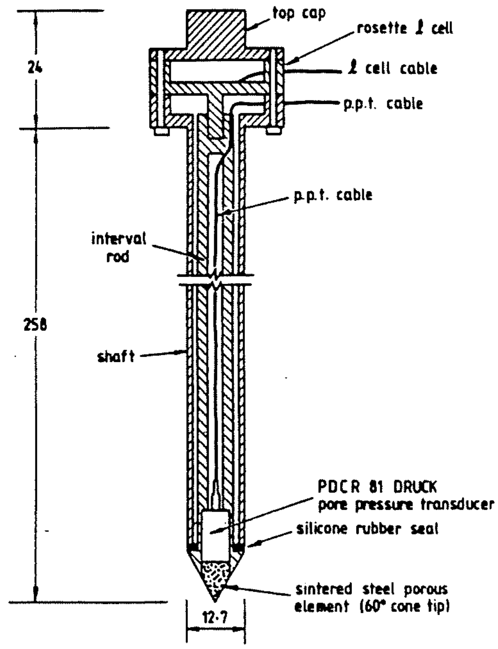

Figure 18b Piezocone
(Almeida, 1984)

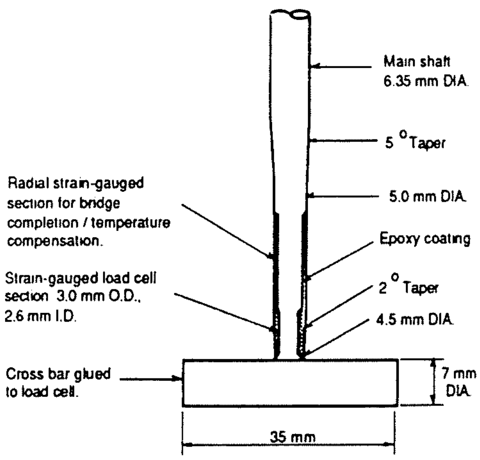

(a) Schematic diagram

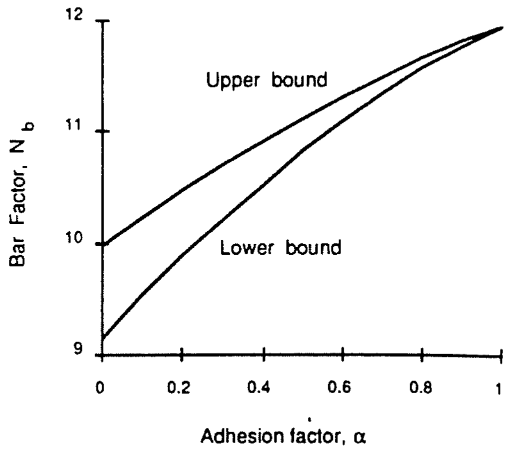

(b) Variation of N_b with surface roughness

Figure 19 Bar penetrometer (Stewart and Randolph, 1991)

Bar penetration testing

A bar penetrometer (Stewart and Randolph, 1991) is a semi-rough cross bar, of length approximately 5 bar diameters d_b (d_b = 7 mm), with smooth ends, mounted on a shaft which has been instrumented to read axial load (Figure 19a). A classical plasticity solution in *plane strain* (Randolph and Houlsby, 1984) may be used to relate the force required to pull or push the cylinder through a rigid-perfectly plastic medium of strength c_u. This fundamental relationship presents significant advantages when predicting c_u from miniature site investigation devices.

Bar factor N_b may be determined from measurement of the force per unit length P acting on the cylinder where surface roughness is equal to αc_u and adhesion factor α is zero for a smooth bar, and unity for bar which is rough enough to mobilise friction up to c_u (Figure 19b):

$$N_b = P / (c_u \, d_b) \tag{19}$$

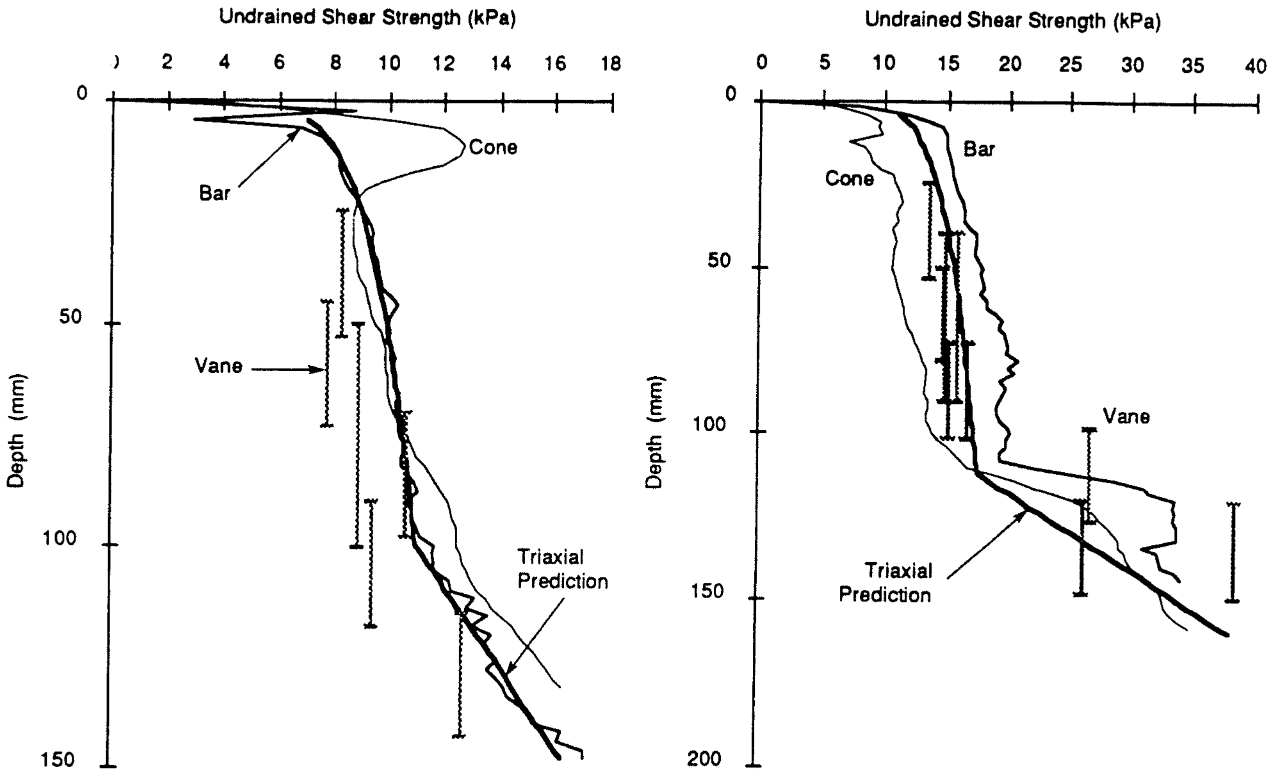

(a) 1 =< OCR < 3

(b) OCR > 3

Figure 20 Comparisons between c_u obtained from in-flight bar and cone penetrometer tests, post-test shear vane tests and predictions based on triaxial data (Stewart and Randolph, 1991)

Comparisons with c_u predicted from in-flight cone penetrometer, post-test vane shear and independent triaxial tests (Stewart and Randolph, 1991) were fair. It was noted that the bar gave a c_u profile which was very similar to the triaxial prediction for normally and lightly overconsolidated samples (Figure 20a) and about 20% greater for OCR > 3 (Figure 20b). The vane shear results would be expected to underpredict the equivalent values at 100g due to ingress of water during deceleration and prior to inserting the vane. The degree by which this occurs is dependent on the time interval and the coefficient of consolidation for the sample.

Whilst the bar diameter needs to be small so that the change in c_u with scaled prototype depth is insignificant, and can be assumed to be constant in the near field to the bar, the end effects of pushing or pulling the bar vertically adjacent to the soil surface or an interface with a stiffer layer must also be considered.

Strain measurement

Radiography

It is common practice to insert mixtures of lead, water and soluble oil into the clay stratum, at the model making stage, using a syringe. Before testing at higher gravities, exposure of a suitable film to X-rays reveals the initial location of these lead threads. Subsequently, the soil deformations caused by the loading sequences will allow post-test examination of these internal movements by identical radiographic techniques. Although it is difficult to quantify these internal strains to a satisfactory degree of accuracy, they do give a useful impression of the soil deformations and also the presence of any rupture zones. Figure 21 shows information from a post-centrifuge model test radiograph of the location of rupture zones caused by the forced subsidence of a model abyssal plain.

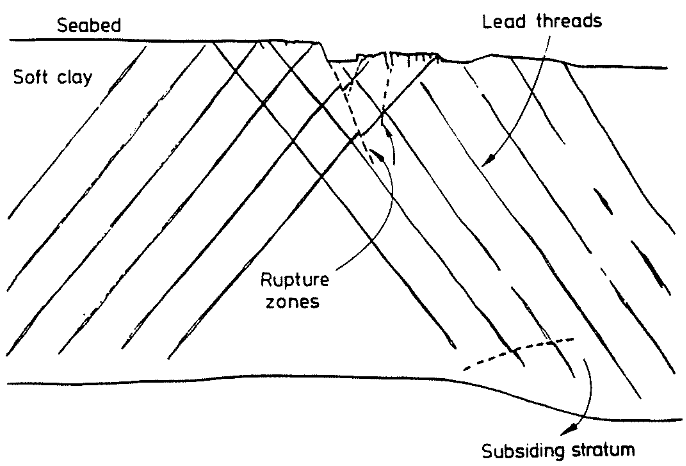

Figure 21 Tracing of a radiograph of diagonal lead threads inserted through an abyssal plain, with a subsiding substratum modelled by collapsing flaps (dashes represent ruptures; Stone, 1988)

Spotchasing

Insertion of black marker 'bullets' may allow evaluation of relative movements at various stages in the loading programme by back analysis of high quality photographs taken in-flight. This technique is known as spotchasing. A classic demonstration of the qualitative use of these procedures is given by Phillips (1990) for installation of an offshore jack up rig near to piles which are intended to support an operational platform.

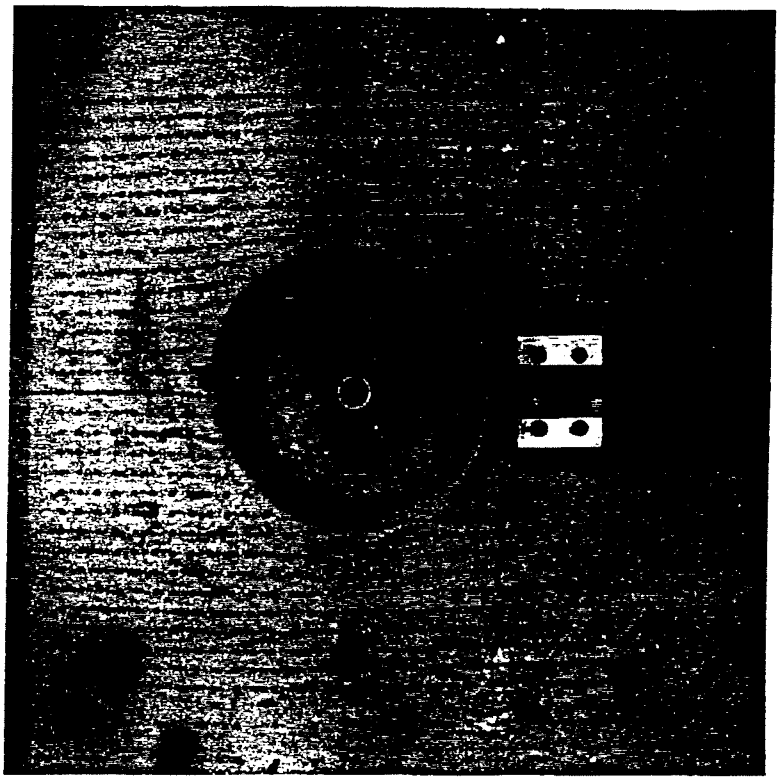

Figure 22 Plan on the spudcan posthole - centrifuge model at 1/100th scale (after Phillips, 1990)

A large diameter spud was driven into soft soil adjacent to a group of piles. A photograph, in plan, of the spudcan posthole and surrounding markers is shown in Figure 22 (Phillips, 1990). Measurement of the differential movements of the markers to find vector displacements (Figure 23) may allow appropriate values to be input into a strain evaluation computer program to estimate contours of shear strain.

In some other cases, it has been possible to derive sufficient information for use in the analysis of geo-structural mechanisms (Bolton and Powrie, 1988; Sun, 1989).

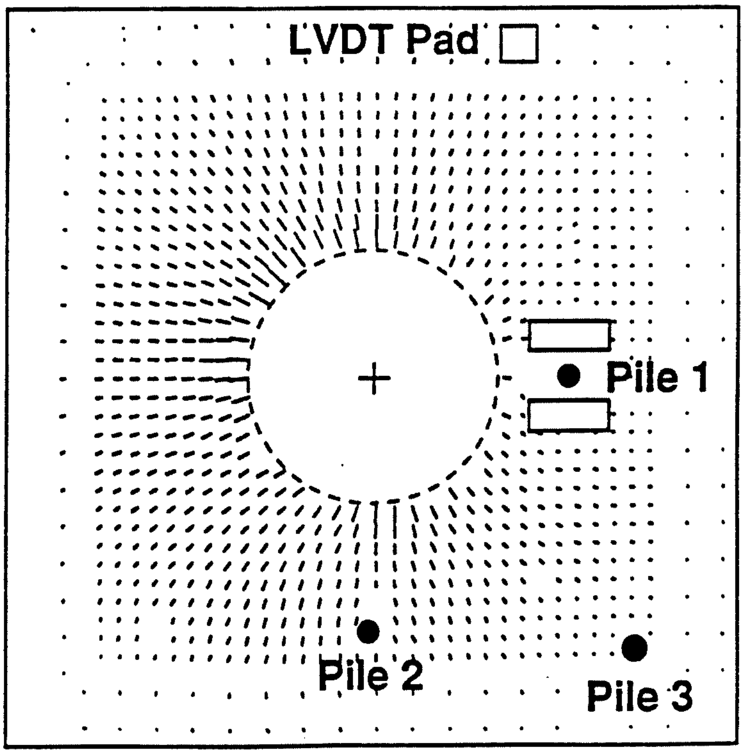

Figure 23 Vectors of outward horizontal movement (after Phillips, 1990)

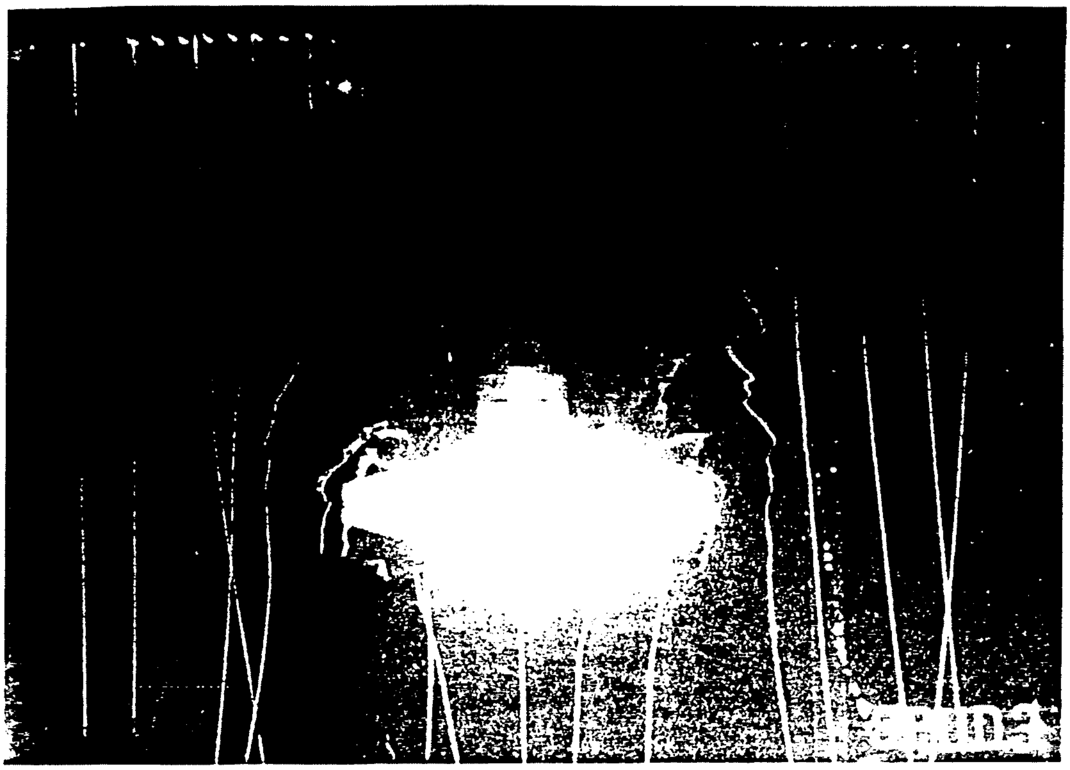

Figure 24 Penetration of a large diameter spud footing adjacent to a pile (after Phillips, 1990)

An X-ray exposure (taken horizontally; Figure 24) shows lead threads inserted vertically into the soil and black markers, which were placed on the surface to outline the relative local deformation of the soil, the spud and the pile. Close to the spud, it is possible to see where the lead threads have been ruptured.

At shallow depths of embedment H of the spud can of diameter B, a Prandtl bearing capacity solution might have been anticipated. However, for a ratio of H/B approaching 1.5, this X-ray clearly shows a different displacement mechanism in which the soil has been extruded upwards past the circumference of the spud, but over a much smaller annulus than might have been predicted. The soil displacement vectors are mainly vertical in this region, and in consequence, the bending moments induced in the pile by soil squeezing past it in a lateral direction were found to have been less than expected.

CONCLUSIONS

Centrifuge model testing is particularly advantageous in investigations of the performance of large scale structures in a marine environment. Appropriate idealisations may be adopted to reveal the key mechanisms of behaviour.

It is possible to create centrifuge models in clay using 'laboratory' soils such as kaolin, according to a prescribed design strength profile.

Variations of the properties of these kaolin based soils may be achieved by the addition of a silt fraction. In particular, strength, stiffness and permeability may be increased, with the added benefit that shear surfaces will not form residual planes of weakness at values of ϕ' much less than ϕ_{crit}'.

A combination of site investigation devices, empirical interpretations and comparisons between in-situ and laboratory data allow determination of soil strength.

Displacement mechanisms may be observed, leading to an evaluation of strains in the soil matrix adjacent to the marine structure.

Stress paths during one dimensional consolidation, model making and testing in-flight may be established.

The influence of recent stress and strain path and the direction of the loading increment may be accounted for in the development and understanding of deformation mechanisms, leading to improved methods of serviceability limit state design.

ACKNOWLEDGEMENTS

The assistance of many members of the Cambridge University Soil Mechanic Group, under the direction of Professor A.N. Schofield FRS, is gratefully acknowledged.

Carol Mozuraitis and Barrie Wilkinson carried out the testing programme on the kaolin-rock flour mix (KRF) soil, and reduced the data.

Jitendra Sharma, Fraser Bransby and Ed Ellis provided further data of consolidation characteristics and shear strengths.

Technical support from Messrs Neil Baker, Steve Chandler, Chris Collison, Paul Ford, John Chandler, Tim Ablett and Adrian Brand was instrumental in the delivery of almost all of the centrifuge test data reported herein.

Carol Mozuraitis, Alan Bailey, Sheila Mason and Marica Lopez helped with the production of figures and assembly of the final manuscript.

Richard Dean and Chrysanthi Savvidou kindly reviewed the text; Malcolm Bolton and Charles Ng provided opportunities for discussion of the contents.

Finally, Ryan Phillips' cooperation in so many areas was vital. In particular, the permission for reproduction of the spud can/pile interaction is gratefully acknowledged.

REFERENCES

Airey, D.W. 1984. Clays in the simple shear apparatus. Cambridge University PhD thesis.

Almeida, M.S.S. 1984. Stage constructed embankments on soft clay. Cambridge University PhD thesis.

Al Tabbaa, A. 1984. Anisotropy of clay. Cambridge University MPhil thesis.

Al Tabbaa, A. 1987. Permeability and stress-strain response of Speswhite Kaolin. Cambridge University PhD thesis.

Bjerrum, L. 1973. Problems of soil mechanics and construction on soft clays and structurally unstable soils. Proc. 8th ICSMFE Moscow, Vol. 3, pp. 111-159.

Blight, G.E. 1968. A note on field vane testing of silty soils. Can. Geot. J. Vol. 5, No. 3, pp. 142-149.

Bolton, M.D. 1991. Geotechnical stress analysis for bridge abutment design. TRRL CR270.

Bolton, M.D. and Powrie, W. 1988. Behaviour of diaphragm walls in clay prior to collapse. Geotechnique 38, No. 2, pp.167-189.

Bolton, M.D., Gui, M.W. and Phillips, R. 1993. Review of miniature soil probes for model tests. 11th SEAGC, Singapore. Preprint.

Bransby, M.F. 1993. Centrifuge test investigation of the buttonhole foundation technique. Data Report. 33p.

Broms, B.B. and Casbarian, A.O. 1965. Effects of rotations of the principal stress axes and of the immediate principal stress on the shear strength. Proc. 6th ICSMFE, Montreal, Vol. 1, pp. 179-183.

Cheah, H. 1981. Site investigation techniques for laboratory soils models. Cambridge University MPhil thesis.

Corte, J.-F., Garnier, J., Cottineau, L.M. and Rault, G. 1991. Determination of model properties in the centrifuge. Centrifuge '91, H.Y.Ko and F.G.McLean (eds). Balkema. pp. 607-614.

Craig, W.H. 1988. Centrifuge models in marine and coastal engineering. Centrifuges in Soil Mechanics, W.H. Craig, R.G. James and A.N. Schofield (eds). Balkema. pp. 149-168.

Craig, W.H. and Chua, K. 1991. Large displacement performance of jack-up spud cans. Centrifuge '91, H.Y.Ko and F.G.McLean (eds). Balkema. pp. 139-144.

Ellis, E.A. 1993. Lateral loading of bridge abutment piles due to soil movement. Cambridge University 1st year Report. 27p.

Fuglsang, L.D. and Steensen-Bach, J.O. 1991. Breakout resistance of suction piles in clay. Centrifuge '91, H.Y.Ko and F.G.McLean (eds). Balkema. pp. 153-160.

Endicott, L.J. 1970. Centrifugal testing of soil models. Cambridge University PhD thesis.

Hamilton, J.M., Phillips, R., Dunnavant, T.W. and Murff, J.D. 1991. Centrifuge study of laterally loaded pile behavior in clay. Centrifuge '91, H.Y.Ko and F.G.McLean (eds). Balkema. pp. 285-293.

Hellawell, E. 1993. Resistivity probes: a review of current practices and an investigation into the properties of different systems. To be published as a CUED Report.

Hensley, P.J. 1989. Accelerated physical modelling of transport processes in soil. Cambridge University PhD thesis.

Horner, J.M. 1982. Centrifugal modelling of multi-layer clay foundations subject to granular embankment loading. King's College, London University PhD thesis.

Kulhawy, F. and Mayne, P. 1990. Manual on estimating soil properties. Report EL-6800. Electric Power Res. Inst., Palo Alto, 306p.

Kutter, B.L. 1982. Centrifugal modelling of the response of clay embankments to earthquakes. Cambridge University PhD thesis.

Kutter, B.L., Sathialingam, N. and Herrmann, L.R. 1988. The effects of local arching and consolidation on pore pressure measurements in clay. Centrifuge '88, J.F. Corte, (ed). Balkema. pp. 115-118.

Lach, P. 1992. Seminar on centrifuge model tests on iceberg scour above pipelines buried in clay, and subject for forthcoming thesis at Memorial University of Newfoundland, St John's, Newfoundland.

Ladd, C.C., Foott, R., Ishihara, K., Schlosser, F. and Poulos, H.J. 1977. Stress-deformation and strength characteristics. Proc. 9th ICSMFE, Tokyo, Vol. 2, pp. 421-494.

Lawrence, D.M. 1980. Some properties associated with kaolinite soils. Cambridge University M. Phil thesis.

Leroui, S., Kabbaj, M., Tavenas, F. and Bouchard, R. 1985. Stress-strain-strain rate relation for the compressibility of sensitive natural clays. Geotechnique 35, Vol. 2, pp. 152-80.

Mahmoud, M. 1988. Vane testing in soft clays. Ground Engineering, Vol. 21, No. 7, pp. 36-40.

Mair, R.J. 1979. Centrifugal modelling of tunnel construction in soft clay. Cambridge University PhD thesis.

Mayne, P.W. and Kulhawy, F. 1982. K_o-OCR relationships in soil. Proc. ASCE, JGED, Vol. 102, pp. 197-228.

Mayne, P.W. 1992. In-situ determination of clay stress history by piezocone. Wroth Memorial Symposium. Oxford. pp. 361-372 (Preprint).

Meigh, A.C. 1987. Cone penetration testing. CIRIA, Butterworths. 137p.

Mesri, G. 1975. Discussion: New design procedure for stability of soft clays. Proc. ASCE, JGED. Vol. 103 GT5. pp. 417-430.

Mozuraitis, C.H. and Springman, S.M. 1993. Properties of a kaolin mix soil. To be published as a CUED Technical Report.

Muir Wood, D. 1990. Soil behaviour and critical state soil mechanics. CUP. 462p.

Nadarajah, V. 1973. Stress-strain properties of lightly overconsolidated clays. Cambridge University PhD thesis.

Nunez, I. 1989. Tension piles in clay. Cambridge University PhD thesis.

Phillips, R. 1988. Centrifuge lateral pile tests in clay. PR-10592. Task 2 & 3 - Final Report to Exxon Production Research. 39p.

Phillips, R. 1990. Spudcan/Pile Interaction Centrifuge Model Test Spud 3 - Final Report. A report to EPR Corp. Houston, TX, USA. Lynxvale Ltd. Cambridge.

Phillips, R. and Valsangkar, A. 1987. An experimental investigation of factors affecting penetration resistance in granular soils in centrifuge modelling. CUED/D TR210. 17p.

Phillips, R. and Gui, M.W. 1992. Cone Penetrometer Testing. Phase 1 Report, In-situ investigation. EEC Contract: SC1-CT91-0676.

Poorooshasb, F. 1988. The dynamic embedment of a heat emitting projectile. Cambridge University PhD thesis.

Powrie, W. 1987. The behaviour of diaphragm walls in clay. Cambridge University PhD thesis.

Randolph, M.F. and Houlsby, G.T. 1984. The limiting pressure on a circular pile loaded laterally in clay. Geotechnique 34, No. 4, pp. 613-623.

Renzi, R., Maggioni, W., Smits, F. and Manes, V. 1991. A centrifugal study on the behavior of suction piles. Centrifuge '91, H.Y.Ko and F.G.McLean (eds). Balkema. pp. 169-177.

Rossato, G., Ninis, N.L. and Jardine, R.J. 1992. Properties of some kaolin-based model clay soils. ASTM GTJODJ, Vol. 15, No. 2, pp. 166-179.

Rowe, P.W. 1975. Displacement and failure modes of model offshore gravity platforms founded on clay. Conf. Offshore Europe '75, pp.218. 1- 17. Spearhead Publications, Aberdeen.

Savvidou, C. 1984. Effects of a heat source in saturated clay. Cambridge University PhD thesis.

Schmidt, B. 1966. Discussion: Earth pressures at rest related to stress history. Can. Geot. J., 3, No. 4, pp. 239-242.

Schmidt, B. 1983. Discussion: K_o-OCR relationships in soil. Mayne, P., Kulhawy, F. 1982. Proc. ASCE, JGED, Vol. 109, pp. 866-867.

Schofield, A.N. and Wroth, C.P. 1968. Critical State Soil Mechanics. McGraw-Hill. 309p.

Schofield, A.N. 1980. Cambridge University Geotechnical Centrifuge Operations. 20th Rankine lecture. Geotechnique 30, No. 3. pp. 227-268.

Sharma, J.S. 1993. Construction of reinforced embankments on soft clay. Forthcoming Cambridge University PhD thesis.

Skempton, A.W. 1957. The planning and design of the new Hong Kong airport. Proc. ICE 7, pp. 305-307.

Sketchley, C.J. 1973. The behaviour of kaolin in plane strain. Cambridge University PhD thesis.

Smith, C.C. 1992. Thaw induced settlement of pipelines in centrifuge model tests. Cambridge University PhD thesis.

Springman, S.M. 1989. Lateral loading on piles due to simulated embankment construction. Cambridge University PhD thesis.

Springman, S.M. 1991. Performance of a single lattice leg under lateral load. EEPUK Report. Contract No. EP-022R, Task Order: 2-022. 23p.

Stewart, D.P. and Randolph, M.F. 1991. A new site investigation tool for the centrifuge. Centrifuge '91, H.Y. Ko and F.G. McLean (eds). Balkema. pp. 531-537.

Stone, K.J.L. 1988. Modelling the rupture development in soils. Cambridge University PhD thesis.

Sun, H.W. 1989. Ground deformation mechanisms for soil-structure interaction. Cambridge University PhD thesis.

Tang, Z. 1993. Laboratory measurement of shear strength and related acoustic properties. MEng thesis, Memorial University of Newfoundland, St John's, Newfoundland.

Tovey, N.K. 1970. Electron microscopy of clays. Cambridge University PhD thesis.

Trak, B., LaRochelle, P., Tavenas, F., Leroueil, S. and Roy, M. 1980. A new approach to the stability analysis of embankments on sensitive clays. Can. Geot. J. 17, Vol. 4, pp. 526-544.

Vinson, T.S. 1982. Ice forces on offshore structures. Proc. Workshop on High Gravity Simulation for Research in Rock Mechanics. Colorado School of Mines. pp. 60-68.

Vinson, T.S. 1983. Centrifugal modelling to determine ice/structure/geologic foundation interactive forces and failure nmechanisms. Proc. 7th Int. Conf. on Port and Ocean Engineering under Arctic Conditions. pp. 845-854.

Waggett, P.R. 1989. The effect of lubricants on the interaction between soils and perspex. Cambridge University Part II Project Report.

Wilkinson, B.J. 1993. An investigation into the effects of adding a substantial granular content to a kaolin based mix. Cambridge University Part II Project Report.

Wong, P.C., Chao, J.C., Murff, J.D., Dean, E.T.R., James, R.G., Schofield, A.N., and Tsukamoto, Y. 1993. Jack-up rig foundation modelling II. Offshore Technology Conference 7303.

Wroth, C.P. 1972. General theories of earth pressures and deformations. Proc. 5th ECSMFE, Madrid, II, pp. 33-52.

Wroth, C.P. 1975. In-situ measurements of initial stresses and deformation characteristics. CUED/D TR23.

Wroth, C.P. 1979. Correlations of some engineering properties of soils. Proc. 2nd Int. Conf. Behaviour of Offshore Structures, London. Vol. 1, pp. 121-132.

Yong, R.N. and McKyes, E. 1971. Yield and failure of clay under triaxial stresses. Proc. ASCE SM 1, pp. 159-176.